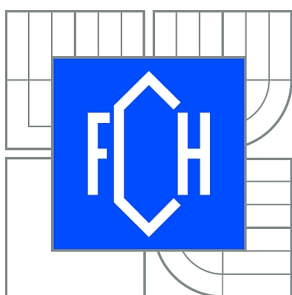




VYSOKÉ UČENÍ TECHNICKÉ V BRNĚ

BRNO UNIVERSITY OF TECHNOLOGY



FAKULTA CHEMICKÁ  
ÚSTAV CHEMIE MATERIÁLŮ

FACULTY OF CHEMISTRY  
INSTITUTE OF MATERIALS SCIENCE

## VLIV SLOŽENÍ NA PEVNOST ADHEZE MEZI ČÁSTICOVÝMI A VLÁKNOVÝMI KOMPOZITY.

EFFECT OF COMPOSITION ON ADHESION STRENGTH BETWEEN PARTICLE FILLED  
COMPOSITE AND FIBER REINFORCED COMPOSITE.

DIZERTAČNÍ PRÁCE

DOCTORAL THESIS

AUTOR PRÁCE

AUTHOR

Ing. RADOSLAV TRAUTMANN

VEDOUCÍ PRÁCE

SUPERVISOR

prof. RNDr. JOSEF JANČÁŘ, CSc.

BRNO 2010

## **ABSTRAKT**

Disertační práce se zabývala vlivem adheze mezi vláknovým (FRC) a částicovým (PFC) kompozitem a složením obou komponent na mechanické vlastnosti a způsob porušování modelových bi-materiálových kompozitních těles při statickém namáhání. Zkoumán byl také vliv způsobu přípravy bi-materiálového kompozitního tělesa na pevnost adheze mezi jeho kompozitními komponentami.

K hodnocení mechanických vlastností bi-materiálových PFC/FRC těles byl použit jak 3 tak 4-bodový ohybový test za pokojové teploty a relativní vlhkosti 70%. Modifikovaný vytrhávací test byl použit k měření smykové pevnosti adheze mezi vláknovým a částicovým kompozitem. Tyto výsledky byly korelovány s výsledky ze strukturní a fraktografické analýzy (TGA, SEM). Experimentální data byla poté analyzována pomocí existujících mikromechanických modelů a byl nalezen vztah mezi tuhostí modelových bi-materiálových těles, složením a geometrií uspořádání jejich komponent a pevností adheze mezi těmito komponentami. Na základě těchto výsledků byl navržen optimální způsob vrstvení a přípravy PFC/FRC bimateriálových těles. Navržené postupy byly použity k přípravě a pre-klinickým testům nosných konstrukcí zubních můstků.

## **ABSTRACT**

This PhD thesis dealt with the influence of adhesion between fiber (FRC) and particulate (PFC) composite and the composition of both components on the mechanical properties and type of fracture of bi-material composite specimens under static loading. The influence of method of preparing a bi-material composite bodies on the strength of adhesion between the composite components was also investigated.

To evaluate the mechanical properties of bi-material PFC / FRC specimens were used as 3 and 4 point bending test at room temperature and relative humidity of 70%. Modified pull-out test was used to measure the shear strength of adhesion between fiber and particulate composite. These results were correlated with the results of structural and fractographic analysis (TGA, SEM). Experimental data were analyzed using existing micromechanical models and found a relationship between stiffness of model bi-material bodies, composition and geometry of the arrangement of their components and adhesion strength between these components. Based on these results, the optimal method of layering and preparation of PFC/FRC bi-material bodies was proposed. The proposed procedures were used for the preparation and pre-clinical tests of frameworks of dental bridges.

## **KLÍČOVÁ SLOVA**

bi-materiálové těleso, částicové kompozity, vláknové kompozity, adheze, 3-bodový ohyb, 4-bodový ohyb, pull-out test

## **KEYWORDS**

bi-material body, particulate composites, fiber reinforced composites, adhesion, 3-point bending test, 4-point bending test, pull-out test

TRAUTMANN, R. Effect of Composition on Adhesion Strength Between Particle Filled Composite and Fiber Reinforced Composite.. Brno: Vysoké učení technické v Brně, Fakulta chemická, 2010. 61 s. Vedoucí dizertační práce prof. RNDr. Josef Jančář, CSc.

### **PROHLÁŠENÍ**

Prohlašuji, že jsem disertační práci vypracoval samostatně a že všechny použité literární zdroje jsem správně a úplně citoval. Disertační práce je z hlediska obsahu majetkem Fakulty chemické VUT v Brně a může být využita ke komerčním účelům jen se souhlasem vedoucího disertační práce a děkana FCH VUT.

.....

### **Acknowledgement**

I would like to thank my supervisor, prof. RNDr. Josef Jančář, CSc. for his help during my work on this thesis and to Jiří Dvořák for the SEM images.

**- CONTENT -**

<b>1</b>	<b>INTRODUCTION .....</b>	<b>5</b>
<b>2</b>	<b>LITERATURE REVIEW .....</b>	<b>6</b>
<b>2.1</b>	<b>MATERIALS IN DENTISTRY.....</b>	<b>6</b>
2.1.1	Polymers .....	6
2.1.1.1	Acrylates and methacrylates.....	6
2.1.1.2	Multifunctional acrylates and methacrylates.....	7
2.1.2	Composites.....	8
2.1.2.1	Particulate composites.....	9
2.1.2.2	Fiber reinforced composites .....	10
<b>2.2</b>	<b>FIBER REINFORCED COMPOSITES.....</b>	<b>12</b>
2.2.1	General remarks .....	12
2.2.2	Glass fibers .....	12
2.2.2.1	E-Glass.....	12
2.2.2.2	S-Glass .....	13
2.2.3	Unidirectional continues fibers reinforced composite .....	14
2.2.4	Laminae .....	14
<b>2.3</b>	<b>ROLE OF INTERPHASE IN FRC.....</b>	<b>16</b>
<b>2.4</b>	<b>BASIC PRINCIPLES OF ADHESION.....</b>	<b>17</b>
2.4.1	Interphase Region.....	17
2.4.2	Chemical Aspect of Adhesion .....	19
2.4.3	Physical Aspect of Adhesion.....	20
2.4.4	Mechanical Aspect of Adhesion.....	22
2.4.5	Interfacial Adhesion in Fiber Reinforced Composites .....	22
<b>3</b>	<b>AIM OF THE THESIS .....</b>	<b>24</b>
<b>4</b>	<b>EXPERIMENTAL .....</b>	<b>25</b>
<b>4.1</b>	<b>MATERIALS USED .....</b>	<b>25</b>
4.1.1	Fiber reinforced composites (FRC) .....	25
4.1.2	Particulate composites (PFC).....	26
<b>4.2</b>	<b>METHODS .....</b>	<b>27</b>
4.2.1	Thermogravimetric analysis .....	27
4.2.2	Shear bond strength tests.....	27
4.2.3	3-point bending tests.....	29
4.2.4	4-point bending tests.....	30
4.2.5	Scanning Electron Microscopy .....	32

<b>4.3</b>	<b>SPECIMEN PREPARATION</b> .....	<b>33</b>
4.3.1	Shear bond strength tests.....	33
4.3.2	3 and 4-point bending tests.....	34
<b>5</b>	<b>RESULTS AND DISCUSSION</b> .....	<b>36</b>
<b>5.1</b>	<b>STRUCTURAL ANALYSIS OF THE FRC</b> .....	<b>36</b>
<b>5.2</b>	<b>MECHANICAL PROPERTIES OF COMPOSITES</b> .....	<b>40</b>
5.2.1	Shear adhesion strength .....	40
5.2.1.1	Samples prepared according schedule A .....	40
5.2.1.2	Samples prepared according schedule B .....	44
5.2.1.3	Samples prepared according schedule C.....	47
5.2.2	Young's modulus and ultimate strength in 3-point bending test.....	50
5.2.2.1	Properties of components .....	50
5.2.2.2	C&B composite reinforced with FRC in different position.....	50
5.2.2.3	C&B composite reinforced with FRC at the bottom .....	52
5.2.3	Young's modulus and ultimate strength in 4-point bending test.....	55
<b>6</b>	<b>CONCLUSIONS</b> .....	<b>57</b>
<b>7</b>	<b>LITERATURE</b> .....	<b>59</b>

# 1 INTRODUCTION

Fiber reinforced materials have been used by a man for a very long time. The first to be used were naturally occurring composites, such as wood, but man also found out, long ago, that there were advantages to be gained from using artificial mixture of materials with one component fibrous such as straw in clay, for bricks, or horse hair in lime plaster for ceilings.

Recently, with the advent of cheap and strong glass fibers, and with the discovery of a number of new fiber-forming materials with better properties than anything available heretofore, the interest in fiber reinforced materials has increased rapidly, and is still accelerating. Fiber reinforced polymers are replacing metals in a whole host of situations where load-carrying capacity is important. More efficient aircraft, turbine engines, and cars, and more durable boats, can be produced with fiber composites, and worthwhile new applications for these materials are being found almost every day [1].

Dentistry represents the new application field for this kind of materials. This study is focused on the effect of reinforcement commonly used particulate dental composites with fiber reinforced composites [2,3] which are in consequence of their unique (tailor-made) properties (high mechanical resistance, unsurpassed aesthetics and relatively simple way of processing) promising materials which could replace present common used ones as metal, metal alloys and porcelain in dentistry. These composites could be used for making of load bearing application in dentistry ex. splints, post-orthodontic retainers and frameworks for adhesively bonded bridges [4].

The main attention is applied on appropriate combination of particulate composite with fiber reinforced composites and on the way how fix these two different materials together to achieve best mechanical properties.

## 2 LITERATURE REVIEW

### 2.1 MATERIALS IN DENTISTRY

Metals and alloys, ceramics, polymers and composites are the four basic groups of materials, which are widely used in dentistry. Whilst metals are used as restorative materials [5] or still less and less for preparation of crowns, inlays, onlays, bridges, etc., the ceramics are routinely used as coatings or veneers to improve the esthetics of metallic dental restorations or as stand-alone veneers for anterior teeth.

On the other hand, polymers and their composites are the fastest developing groups of dental materials. Combination of appropriate matrices with appropriate fillers enables preparation of tailor-made materials for specific applications. They are used for production of dentures, adhesive agents enhancing the bonding between various materials and tooth structure and as anterior or posterior restorative materials [4].

#### 2.1.1 Polymers

Rubber, celluloid, Bakelite, polystyrene and poly(vinyl chloride) were the first polymers introduced to dentistry in the second part of the 19<sup>th</sup> and at the beginning of the 20<sup>th</sup> century. These materials were used for preparation of dentures. However, insufficient aesthetics and difficult way of processing were the main disadvantages of their wider use.

These problems were solved during the late 1940s and the early 1950s when acrylate polymers were introduced to dentistry. Since thermoplastic acrylates, like poly(methyl methacrylate) and thermosetting dimethacrylates (bis-GMA, TEGDMA, UEDMA) are used for preparation of dentures and as the matrices of dental composites in restorative dentistry, respectively [6].

##### 2.1.1.1 Acrylates and methacrylates

Methyl methacrylate (MMA) and poly(methyl methacrylate) are two the most important acrylates in dentistry. MMA is a clear transparent liquid at room temperature. It exhibits a high vapor pressure and is an excellent organic solvent.

Poly(methyl methacrylate) (Fig. 1) is a transparent resin of remarkable clarity. The resin is extremely stable. It does not discolor in ultraviolet light, and it exhibits remarkable aging properties. It is chemically stable to heat and softens at 125°C, and it can be molded as a thermoplastic material.

Like all acrylic resins, poly(methyl methacrylate) exhibits a tendency to absorb water. Its amorphous structure possesses a high internal energy; thus, molecular diffusion can occur into the

resin, because less activation energy is required. Furthermore, the polar carboxyl group, even though esterified, can form a hydrogen bridge to a limited extent with water. Because both absorption and adsorption are involved, the term sorption is usually used to describe the total phenomenon. Typical dental methacrylate resins show an increase of approximately 0.5 wt.% after 1 week in water.

The sorption of water is nearly independent of temperature from 0°C to 60°C, but is markedly affected by the molecular weight of the polymer. The greater the molecular weight, the smaller the weight increases. Sorption is reversible if the resin is dried [6 - 7].

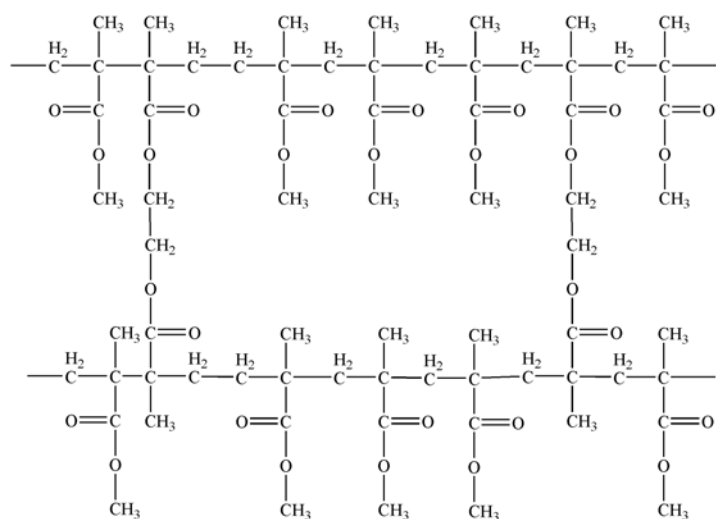


**Figure 1:** PMMA lightly cross-linked by EGDMA [8].

### 2.1.1.2 Multifunctional acrylates and methacrylates

One of the first multifunctional methacrylates used in dentistry was Bowen's resin, bis-GMA (Fig. 2a). The bis-GMA resin can be described as an aromatic ester of a dimethacrylate, synthesized from an ethylene glycol of bis-phenol A and methyl methacrylate. Pure bis-GMA becomes extremely viscous, because has a rigid central structure and two -OH groups. To reduce the viscosity, a low - viscosity dimethacrylate such as TEGDMA (Fig. 2b) is added. Another disadvantage of this monomer is its hydrophilic behavior and the ability to create hydrogen bonds.

The rigidity of the bis-GMA molecule reduces its ability to rotate during polymerization and to participate efficiently in the polymerization process. Therefore, one of the methacrylate groups reacts often, whereas the other does not. This process results in bis-GMA molecule that forms a branch along the polymer chain. Some of these branches cross - linking with adjacent chains; some do not [9].

To reduce the viscosity and increase the degree of conversion, different dimethacrylate resin combinations have been explored through the years. One resin group that has shown some promise is UEDMA (Fig. 2c). This group can be described as any monomer chain containing one or more urethane groups and two methacrylate groups. [6]. This monomer has its self also high viscosity which must be reduced by adding a low viscosity monomer (ex. TEGDMA).

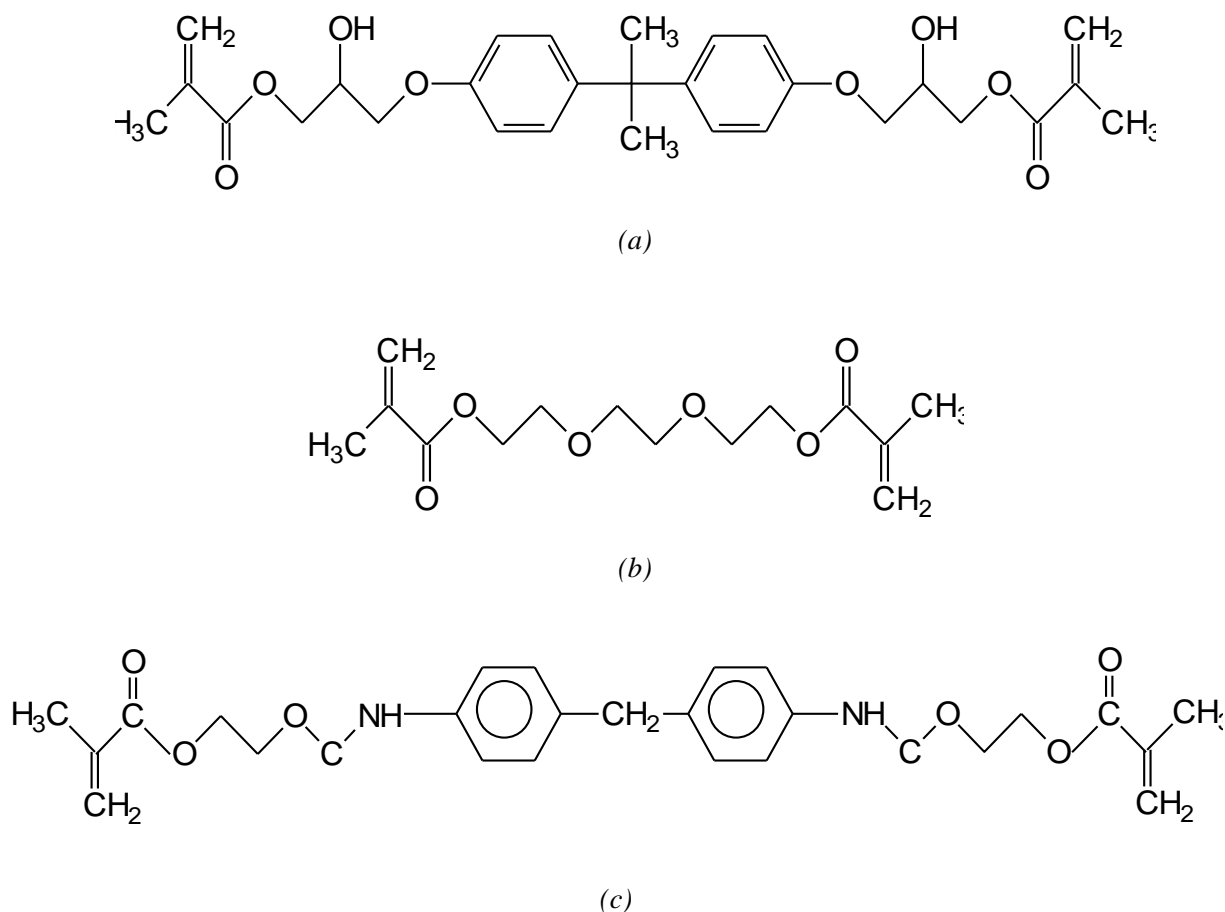


**Figure 2:** The two resins bis-GMA (a) and UEDMA (c) are used as base resin, whereas TEGDMA (b) is used as a diluent to reduce the viscosity of the base resin, particularly that of bis-GMA.

### 2.1.2 Composites

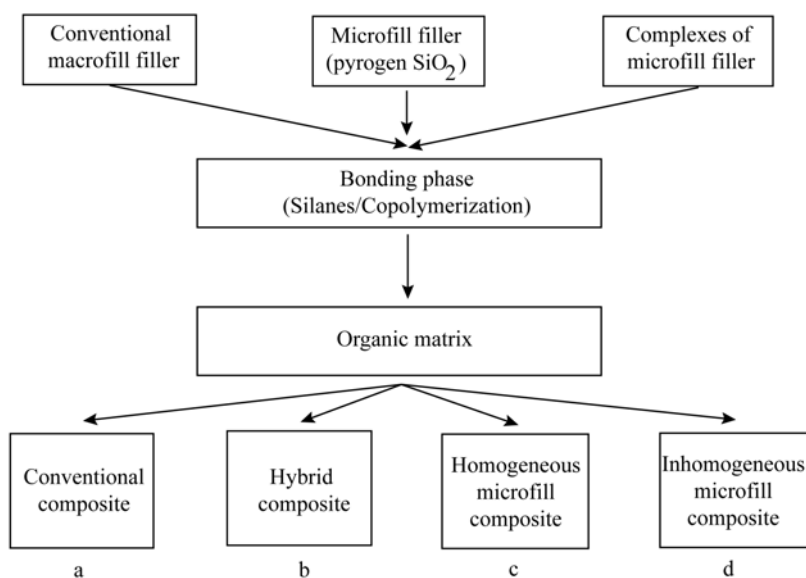
To overcome the disadvantages of unfilled acrylate and dimethacrylate matrices, the particulate and fiber reinforced composites were introduced to dentistry. Since the early 1970s, the resin-based particle composite systems and their dimethacrylate resins have been used for tooth restoration, such as pit and fissure sealants, dentin bonding agents, luting cements for fixed restorations and veneering materials. On the other hand, short or long fiber reinforced low cross-

linked polymethacrylate was used for preparation of fixed dentures and removable appliances [10 - 12].

### 2.1.2.1 Particulate composites

Dental particulate composites are generally composed from three components. Firstly, the matrix, consisting of organic polymer matrix, pigments, viscosity controllers, polymerization initiators, accelerators and inhibitors. Secondly, from the dispersed phase consisting of inorganic fillers, like silica; and thirdly, interphase consisting from the coupling agent, which adheres to both the inorganic filler and matrix. The physical and mechanical properties of the composites are defined by the specific resin matrix used and the nature and degree of the inorganic filler added. The strength and chemical stability of the interfacial bond between filler and resin greatly determine the clinical behavior of the composite material [13].

There exist a number of classification systems of particulate composites in dentistry. System based on the mean particle size of the filler was used in this work for particle composites classification. According to this system, the particle composites are divided on conventional, hybrid, homogeneous micro-filled and non-homogeneous micro-filled (Fig. 3) [14].



- a) Conventional composite with silica, glass or ceramic macro particles. The dimensions of the particles are in a range from  $5\mu\text{m}$  to  $10\mu\text{m}$ .
- b) Hybrid composite with macro- and micro  $\text{SiO}_2$  particles. The average dimension of the particles is in the range from  $2\mu\text{m}$  to  $10\mu\text{m}$ .
- c) Homogeneous microfill composite with dimension of the particles in the range from  $0.01\mu\text{m}$  to  $0.04\mu\text{m}$ .
- d) Inhomogeneous microfill composites with agglomerates in the range from  $100\mu\text{m}$  to  $200\mu\text{m}$ .

**Figure 3:** Classification of particle composites used in dentistry [14].

### 2.1.2.2 Fiber reinforced composites

Fiber reinforced composite (FRC) is a combination of fibers and resin matrix. The effectiveness of fiber reinforcement is depending on many variables including the fiber volume fraction [15], length of fibers [15 - 16], form of fibers [17 - 18], direction of fibers [19 - 21], adhesion of fibers to the polymer matrix [22] and the impregnation of fibers with resin [23]. The fiber composites in dentistry can be divided into two groups. The continuous fiber reinforced dimethacrylate resins are usually used in restorative dentistry for preparation of minimally invasive bridges, oral and vestibular splints, post-orthodontic retainers, space maintainers, etc. The second group of dental composites represents the short-fiber ones. These composites are usually used for preparation of fixed dentures and removable appliances.

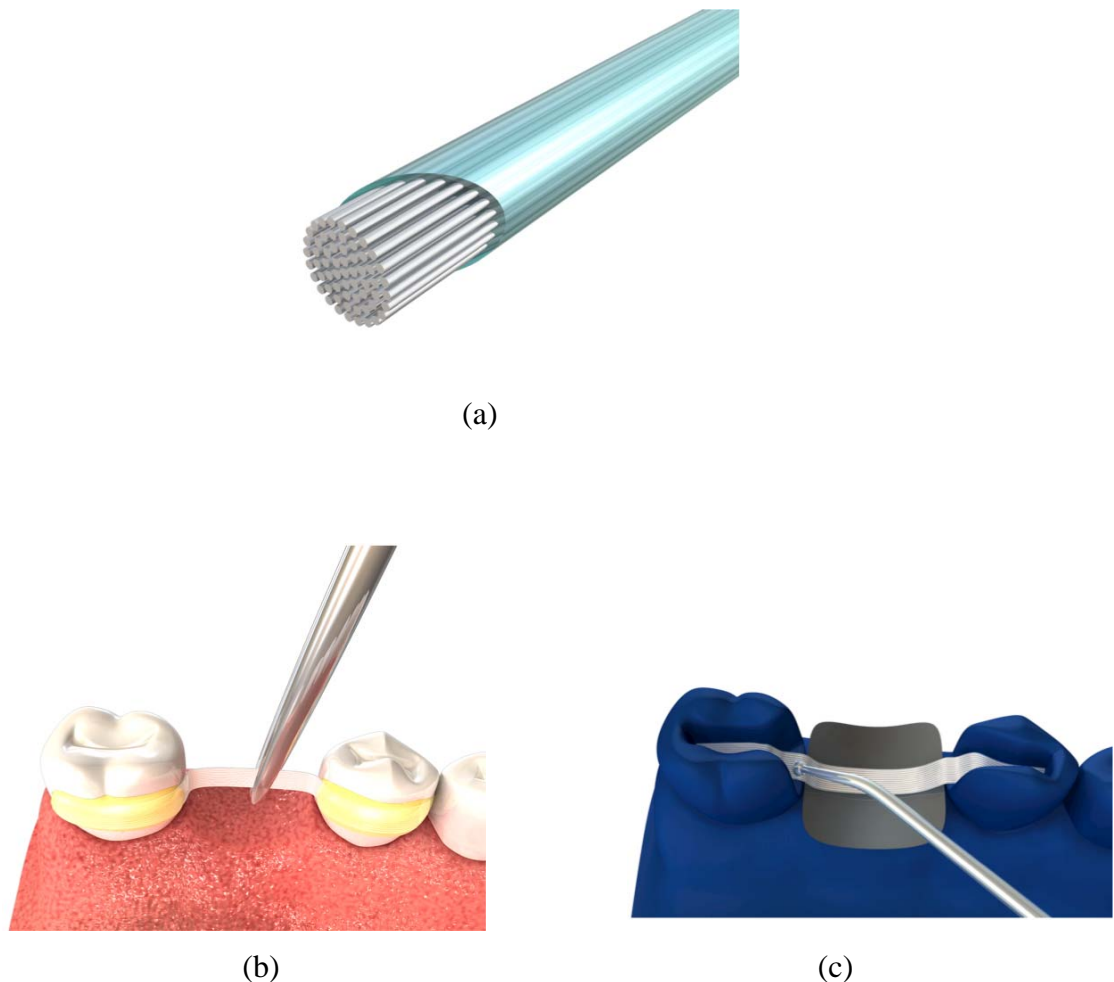
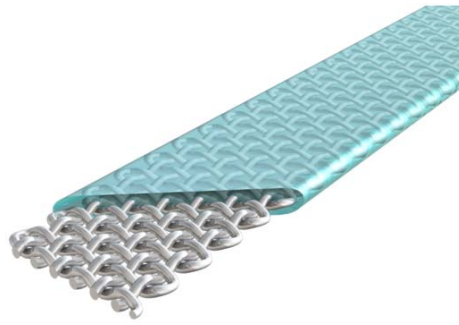
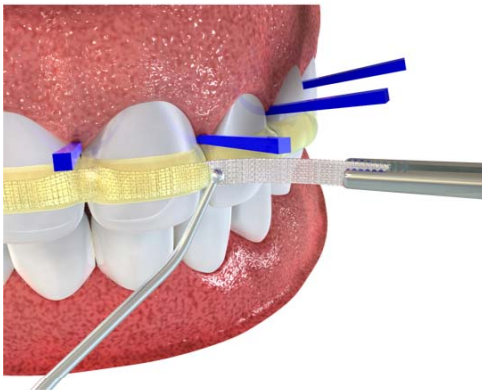


**Figure 4:** Fiber reinforced composite strip with unidirectional reinforcement (a) which can be used for example as space maintainer (b) or as a framework for inlay bridge.



(a)



(b)



(c)

**Figure 5:** Fiber reinforced composite strip with multidirectional reinforcement (a) which can be used for example as vestibular splint (b) or as a framework for Maryland bridge.

## **2.2 FIBER REINFORCED COMPOSITES**

### **2.2.1 General remarks**

Composites are formed by at least two components where at least one discontinuous is phase immersed in a continuous phase or component. The discontinuous component is usually stiffer and more tenacious than the continuous one and it is called reinforcement. The continuous component is called matrix. The matrix can be metallic, ceramic or polymeric. The matrices protect reinforcing fibers, bind them together, and transfer loads to the fibers in the vicinity of fiber breaks via fiber / matrix adhesion. Fibers with high moduli and strength are used in composites as the primary load bearing constituents. In polymer matrix composite, the common fiber reinforcement include glass, carbon, and polymer fibers [24]. In recent years, ceramic fibers have been increasingly utilized to replace glass fibers in some demanding applications.

Composites consisting of two or more different types of fibers in one or more types of matrices are commonly known as hybrid composite. By hybridizing two or more types of fiber in a matrix allows a closer tailoring of composite properties to satisfy specific requirements compared with composite with only a single type of fiber. The purpose of hybridisation is to obtain material retaining the advantages of its components, and overcoming some of their disadvantages. Another desired achievement is related to the cost, being one of the components generally cheaper than the other one.

### **2.2.2 Glass fibers**

The glass fibers used as reinforcement are divided regarding their composition into 3 groups.

#### *2.2.2.1 E-Glass*

For reinforcement purposes, one of the most commonly used glasses is E-glass, developed originally for its good electrical properties [25].

The fibers are usually made by melting and stirring the ingredients, then allowing the liquid to fall through holes 1-2 mm in diameter in a heated platinum plate. The is pulled away rapidly to draw the fibers down to about 10 microns diameter. The platinum plate contains several hundred holes, and the fibers are all drawn together. To obtain strong fibers it is essential that the fiber surfaces do not touch anything, even another fiber. Consequently, they are coated, before being drawn together, with a “sizing”. This usually a starch-oil emulsion, or alternatively a special coating to ensure good adhesion between fiber and matrix when the fibers are later incorporated in a polymer [26].

### 2.2.2.2 S-Glass

A glass which was developed specifically for high strength and modulus is called S-glass. It retains its strength better at high temperatures than does E-glass, as well as having better properties at room temperature. The major constituents of this the E-glass and S-glass are shown in Table 1, respectively. Both S-glass and E-glass are weakened by water but S-glass is more resistant to acids, and less resistant to strong alkaline solutions.

All glass fibers are extremely sensitive to surface damage. Merely touching one fiber against another is sufficient to cause a crack which can reduce the strength to less than a half of the undamaged value. Handling the fibers is only possible if they have a protective layer on them, and even then considerable reduction in strength can occur unless great care is taken [26, 27].

**Table 1:** Composition and properties of glass fibers

	<b>E-glass</b>	<b>S-glass</b>
<i>Composition [wt%]</i>		
SiO <sub>2</sub>	52.4	64.4
Al <sub>2</sub> O <sub>3</sub> +Fe <sub>2</sub> O <sub>3</sub>	14.4	25.0
CaO	17.2	-
MgO	4.6	10.3
Na <sub>2</sub> O+K <sub>2</sub> O	0.8	0.3
B <sub>2</sub> O <sub>3</sub>	10.6	-
BaO	-	-
<i>Properties</i>		
ρ [kg.m <sup>-3</sup> ]	2.6	2.5
K [W.m <sup>-1</sup> .K <sup>-1</sup> ]	13.0	13.0
α [10 <sup>-6</sup> .K <sup>-1</sup> ]	4.9	5.6
σ [GPa]	3.5	4.6
E [GPa]	76.0	85.5
T <sub>max</sub> [°C]	550.0	650.0

### 2.2.3 Unidirectional continuous fibers reinforced composite

One of the most useful forms of composite for the construction of high-performance structural elements is the lamina, made from aligned fiber tapes, containing also partly polymerized matrix. The tapes are also made with woven fibers; these have inferior stiffness, and can not have such high fiber volume fractions, but are generally more tougher than aligned fiber ones.

### 2.2.4 Laminae

Classical aligned fibers lamina is shown on Figure 6. Such laminae are the building blocks used to make high-performance structure elements. An understanding of their properties is essential if we are to analyze structures made from them.

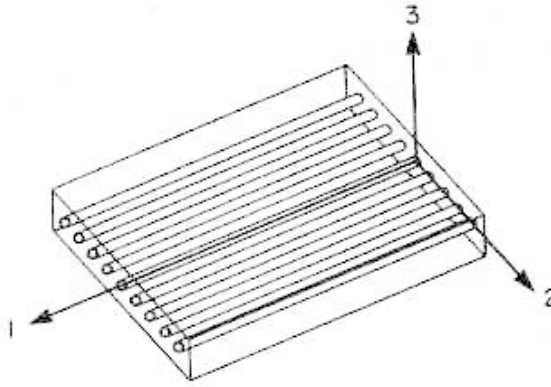


*Figure 6: Axes used for aligned fiber lamina*

For laminae we can assume that plane stress conditions apply. The plain stress state is defined by

$$\sigma_3 = \tau_{23} = \tau_{31} = 0 . \quad (1)$$

Strain are still present normal to the plane of the lamina:

$$\varepsilon_3 = S_{13}\sigma_1 + S_{23}\sigma_2 . \quad (2)$$

The in-plane strain-stress relations we can write in the form

$$\begin{bmatrix} \varepsilon_1 \\ \varepsilon_2 \\ \gamma_{12} \end{bmatrix} = \begin{bmatrix} S_{11} & S_{12} & 0 \\ S_{21} & S_{22} & 0 \\ 0 & 0 & S_{66} \end{bmatrix} \begin{bmatrix} \sigma_1 \\ \sigma_2 \\ \tau_{12} \end{bmatrix} \quad (3)$$

Engineering constants can be used in place of the compliances  $S_{11}$ ,  $S_{12}$ ,  $S_{22}$ , and  $S_{66}$ . They are given in equation (18).

$$[S_{ij}] = \begin{bmatrix} \frac{1}{E_1} & \frac{-\nu_{12}}{E_1} & \frac{-\nu_{13}}{E_1} & 0 & 0 & 0 \\ \frac{-\nu_{12}}{E_1} & \frac{1}{E_2} & \frac{-\nu_{23}}{E_2} & 0 & 0 & 0 \\ \frac{-\nu_{13}}{E_1} & \frac{-\nu_{23}}{E_2} & \frac{1}{E_3} & 0 & 0 & 0 \\ 0 & 0 & 0 & \frac{1}{G_{23}} & 0 & 0 \\ 0 & 0 & 0 & 0 & \frac{1}{G_{31}} & 0 \\ 0 & 0 & 0 & 0 & 0 & \frac{1}{G_{12}} \end{bmatrix} \quad (4)$$

The strain-stress relations can be inverted using reduced stiffness,  $Q_{ij}$ .

$$\begin{bmatrix} \sigma_1 \\ \sigma_2 \\ \tau_{12} \end{bmatrix} = \begin{bmatrix} Q_{11} & Q_{12} & 0 \\ Q_{12} & Q_{22} & 0 \\ 0 & 0 & Q_{66} \end{bmatrix} \cdot \begin{bmatrix} \varepsilon_1 \\ \varepsilon_2 \\ \gamma_{12} \end{bmatrix} \quad (5)$$

$$Q_{11} = \frac{S_{22}}{S_{11}S_{22} - S_{12}^2} = \frac{E_1}{1 - \nu_{12}\nu_{21}} \quad (6)$$

$$Q_{12} = \frac{S_{12}}{S_{11}S_{12} - S_{12}^2} = \frac{\nu_{12}E_2}{1 - \nu_{12}\nu_{21}} \quad (7)$$

$$Q_{22} = \frac{S_{11}}{S_{11}S_{22} - S_{12}^2} = \frac{E_2}{1 - \nu_{12}\nu_{21}} \quad (8)$$

$$Q_{66} = \frac{1}{S_{66}} = G_{12} \quad (9)$$

In practice  $\nu_{12}\nu_{21}$  is usually very small and can be neglected ( $\nu_{12}\nu_{21} = \nu_{12}^2 E_2 / E_1$ ) [1].

### 2.3 ROLE OF INTERPHASE IN FRC

Long fiber reinforced composites comprises of strong fibers which are embed in a relatively week polymer matrix. The function of the matrix is to protect usually brittle fibers from the negative influence of environment and to transfer the load to the fibers. This is done via thin layer between the fibers and the matrix called interphase.

The thin organic layer (interphase) is always presented between the fiber surface and matrix bulk. In industrial FRCs with fiber volume fraction about 0.6 and more, the total volume of this interphase is greater than the volume fraction of the matrix.

The 2D interface and 3D interphase play an important role in determining mechanical and physical properties of composite materials [1, 26, 28-30]. The „interface“ is a hypothetical 2D plane separating two dissimilar phases or components [31]. The „interphase“ is a 3D region of finite located at the fiber/matrix interface with properties different from either fiber or matrix. This region is formed as a result of bonding and reaction between the fiber and the matrix. The interphase structure has gradients in physical properties that greatly influence the performance of the final composite. The definitions of the interface and interphase are schematically illustrated in Fig. 7.

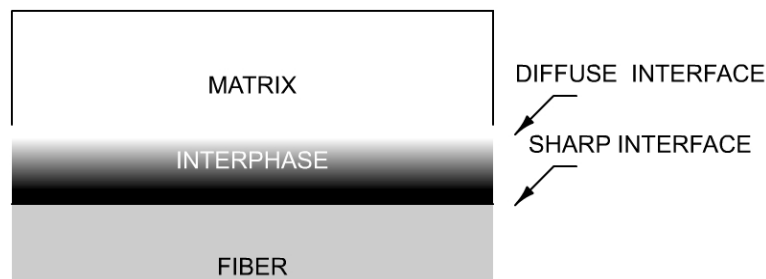


**Figure 7:** Conceptual drawing of interface and interphase in fiber reinforced composites.

## **2.4 BASIC PRINCIPLES OF ADHESION**

Adhesion refers to the state in which two dissimilar bodies are held together by intimate interfacial contact such that mechanical force or work can be transferred across the interface [32-34]. Adhesion between the components is one of the principal factors which affect properties of polymer composites.

Fundamental adhesion occurs through the action of molecular forces and can be characterized by the value of the thermodynamic work of adhesion  $W_a$  required to separate, under equilibrium conditions, a unit area of two contacting dissimilar phases. However, practical adhesion depends not only on molecular interaction, but also on conditions of adhesive joint formation, mechanical properties of the components, shape and size of specimens, pattern of mechanical loading, and other factors.

Thus, the principles of adhesion are very complex, involving chemical, physical and mechanical aspects [35,36].

### **2.4.1 Interphase Region**

In composites, an interphase forms spontaneously even in the absence of fiber surface treatment due to solidification and preferential adsorption. However, some sort of treatment is always used in continuous fiber reinforced composites, which invariably leads to the formation of an interphase with a very complex structure [53].

The properties and thickness of the interphase have significant influence on the interfacial stress, displacement and fracture toughness of fibrous composites [57,62]. Williams et al. [63] proposed that the measurement of modulus in this region is affected by two competing phenomena: a chemical and mechanical effect. The presence of a stiff fiber adjacent to the interphase contributes to the measurement of a high modulus. The chemistry of the matrix contributes to a lower modulus.

The chemical bonding theory explains successfully many phenomena observed for composite made with silane treated glass fibers. However, a layer of silane coupling agent usually does not produce an optimum mechanical strength and must be other important mechanism taking place at the interphase region. An established view is that bonding through silane coupling agent by other than simple chemical reactivity are best explained by interdiffusion and interpenetrating network formation at the interphase region. Interpenetrating polymer network may be considered as mixtures of two or more network polymers, or of network and linear polymer (semi- or pseudo-

interpenetrating polymer network) and at least one of which is synthesized and / or crosslinked in the presence of the other [36,64]. The production of interpenetrating polymer network may be considered as a method of blending polymers which cannot be mixed by conventional procedures because the network polymers cannot be melted or dissolved [36]. Interpenetrating polymer network can be formed sequentially, where a polymer is swollen with a monomer which is then crosslinked, or they can be formed simultaneously where two kinds of monomers are mixed together and crosslinked at the same time [64]. The sequential interpenetrating network that is formed by silane condensation on the fiber surface followed by resin diffusion and subsequent crosslinking should have a pronounced effect on interphase properties [65]. The synergism of two major bonding mechanisms: the chemical reaction and the interpenetrating network theories, is of particular importance in composites containing thermoset matrix [66]. Hence, interdiffusion, crosslinking and interpenetrating polymer network are important factors for initial interfacial strength and retention of moisture resistance [67,68].

DiBenedetto et al. [62,69-71] investigated diffusion and chemical reaction between siloxane coatings (condensed coatings of vinyltrichlorosilane, octenyltrichlorosilane and  $\gamma$ -methacryloxypropyltrichlorosilane on a germanium crystal were used) and an unsaturated polyester. Strong interpenetrating network was formed by interdiffusing and coreacting from the  $\gamma$ -methacryloxypropyltrichlorosilane coatings and the polyester. The vinyltrichlorosilane condenses to a highly crosslinked, relatively impermeable siloxane. The polyester did not diffuse into the network, but probably coreacted at the polyester vinyltrichlorosilane interface. When octenyltrichlorosilane was used, the polyester diffused into the condensing octenyltrichlorosilane film and probably coreacted near the octenyltrichlorosilane-polyester interface. According to results, the interfacial strength was dependent upon siloxane film thickness and crosslink density. Beyond an optimum film thickness, a weak boundary layer reduced the interfacial strength. An increased crosslink density limited interdiffusion and sometimes reduced the bond strength.

Harding et al. [16] used a series of organofunctional silanes with different functionality and length coating on glass particles in polyvinylbutyral matrix. Varied time-temperature profiles during bond formation were found to have no effect on the level of adhesion promotion, indicating that interdiffusion between the polymer and polymerized silane film and formation of an interpenetrating network is not a significant contributor to bond strength. Profound effects were observed with differences in compatibility and length of the silane organofunctional group. Compatibility between the polymer and organofunctional group resulted in high interfacial strength via the formation of Lewis acid-base adducts and molecular overlap. The results indicate

that optimal adhesion promotion for the case of noncovalently bonding silane against an amorphous polymer is obtained with monolayer coverage of organofunctional silane.

### 2.4.2 Chemical Aspect of Adhesion

The chemical bonding theory of adhesion invokes the formation of covalent, ionic or hydrogen bonds across the interface. These can be represented, as in Fig. 8, by new A-B bonds being formed as a result of interfacial chemical reaction. If one material is a solid, such as a fiber or filler, these bonds can be formed by direct reaction between substrate and polymer matrix or due to coupling agents, which react with substrate surface and matrix [37].

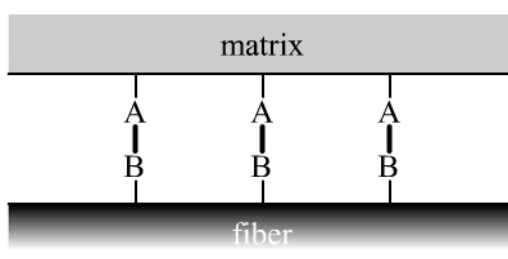


*Figure 8. Interfacial bonds formed by chemical reactions [38]*

### 2.4.3 Physical Aspect of Adhesion

Adhesion is defined thermodynamically by the change in surface free energy when two materials come into contact [39]. The first step in the formation of an adhesive bond is the establishment of interfacial molecular contact by wetting [32]. Adhesion is a steady or firm attachment of two bodies, and as such it can be characterized by the thermodynamic work of adhesion - the work which is needed to separate reversibly two different bodies in contact with each other under equilibrium conditions. Initial premises for the thermodynamic description of adhesion are the characteristics of two bodies: for liquid / solid case - the surface tension of liquid ( $\gamma_l$ ) and solid ( $\gamma_s$ ), and interfacial tension ( $\gamma_{ls}$ ) at the interface between the two bodies in contact [36,40]. Work of adhesion  $W_a$  can be expressed as:

$$W_a = \gamma_s + \gamma_l - \gamma_{ls} \quad (10)$$

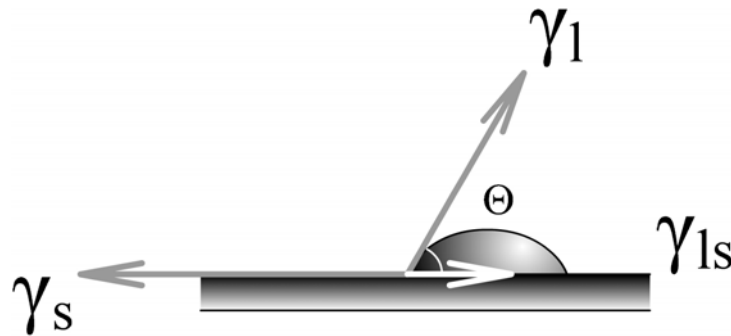


*Figure 9: Forces acting at the circumference of a liquid drop on solid surface.*

On wetting, a drop of liquid forms a definite contact angle  $\theta$  on the solid. The forces in the drop are balanced as shown in Fig. 9. These forces include the tendency of the drop to minimize its surface area by forming a sphere, and the tendency to spread on the solid surface and thus increase the extent of interfacial contact [39]. The state of mechanical equilibrium of the drop on the surface is determined by the relationship known as Young's equation:

$$\gamma_s = \gamma_{ls} + \gamma_l \cdot \cos\theta \quad (11)$$

The joint solution of equations 10 and 11 gives the thermodynamic work of adhesion between liquid and solid:

$$W_a = \gamma_l (1 + \cos \theta) \quad (12)$$

which is Dupre-Young's equation. Spontaneous wetting occurs when  $\Theta = 0$ , or when: [40]

$$\gamma_s \geq \gamma_{ls} + \gamma_l \quad (13)$$

At  $\Theta = 0$ , the behavior of drop is determined by the condition:

$$W_a = 2 \cdot \gamma_l \quad (14)$$

In this case, the drop of liquid spreads on the surface. Good wetting is the important condition for providing high adhesion.

The difference in surface tensions causes the drop to start to spread, which is given by [36]:

$$S = \gamma_s - \gamma_{ls} - \gamma_l \quad (15)$$

The spreading coefficient S is equal to the difference in the work of adhesion and cohesion of liquid [32]:

$$S = W_a = 2 \cdot \gamma_l \quad (16)$$

A positive value of spreading coefficient is the condition for good spreading.

#### 2.4.4 Mechanical Aspect of Adhesion

The mechanical interlocking theory assumes that adhesion is due to irregularities on the surface into which the liquid material can penetrate [39]. Surface roughness may increase the adhesive bond strength by increasing the surface area, promoting wetting, or providing mechanical anchoring sites [32].

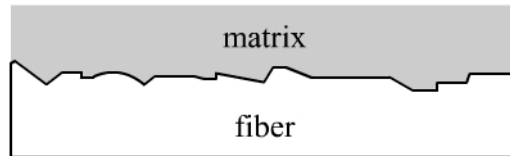


*Figure 10: Interfacial bonds formed by mechanical keying [40].*

#### 2.4.5 Interfacial Adhesion in Fiber Reinforced Composites

The primary function of the composite interphase is to transmit stress from weak polymer matrix to the high strength fibers [42-45]. Adhesion will result in stress transfer between fiber and matrix. The matrix, thus, acts to transfer stress between adjacent fibers. Stress transfer from matrix to fiber occurs, when single fiber composite with ductile matrix is loaded along fiber axis - L. This process is shown in Fig. 11, where  $\sigma$  is the shear stress in the matrix,  $\tau$  is the axial stress in the fiber [46-50].

Adhesion in the interphase region of composite is often ascribed to the following mechanisms: mechanical interlocking, physic-chemical interactions, chemical bonding, and mechanical deformation of the fiber / matrix interphase region [51,52].

Interfacial interactions and interphases play a key role in all multicomponent materials irrespectively of the number and type of their components or their structure. They are equally important in particulate filled or fiber reinforced composites, polymer blends, nanocomposites or biomedical materials [53].

Fiber reinforced composites can be considered at four structural levels. At the molecular level, the interaction between the two dissimilar phases, the fiber and the matrix, is determined by chemical structure of both components and is due to van der Waals forces, acid-base interactions and chemical bonds. From the chemical point of view, the strength of interfacial interaction depends on the surface concentration of interfacial bonds and the bond energies. Quantitatively, it is characterized by the work of adhesion, which includes the contributions of all types of physical and chemical interactions (acid-base, covalent and van der Waals forces). At the micro level (single fibers), interfacial interaction is usually described by global terms which characterize load

transfer from matrix to fibers: bond strength, interfacial shear stress, critical strain energy release rate, etc. The meso level takes into account the actual distribution of reinforcing fibers in the matrix and determines the structural element of the composite. Finally, the macro level characterizes the composite as a bulk material [55].

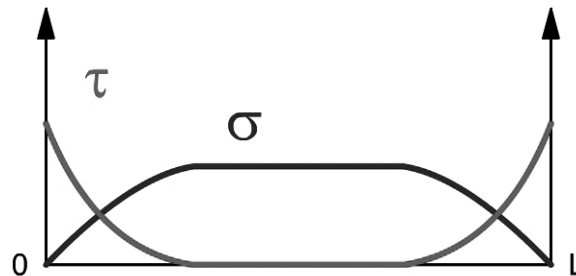


**Figure 11:** Tensile and shear stress profiles along a fiber of length  $L$  [54].

Good adhesion between components is one of the conditions of the application of fiber reinforced composites. Already this statement is a much discussed question. Perfect adhesion is necessary but not sufficient condition to transfer load from the matrix to the fiber. A strong interface bond yields a brittle and notch-sensitive composite and, on the contrary, a weaker interface results in a higher fracture toughness composite [56-59]. Without adhesion the principle of fiber reinforced systems would not work, because the strong fiber carries the load, while the matrix distributes it and transfers from one fiber to the other. The opinion is often expressed that an excessively strong interface leads to a rigid composite, while in the case of weak adhesion the above mentioned principle does not work, thus the strength of adhesion must be set to an optimum value [53].

Most thermosetting polymers possess relatively good adhesion to glass and carbon fiber surfaces, which results in brittle fracture and low impact resistance of these composites. Interphases are created in thermosetting polymers in a specific way: preferential adsorption on the fiber surface of one component of matrix composition and possible chemical bonding at the interface are very important [60]. Control over these processes assumes knowledge of the structure and properties of the formed interphase [61].

### **3 AIM OF THE THESIS**

The main aim of this thesis was to investigate the influence of interfacial adhesion, composition and spatial arrangement of particulate filled (PFC) and fiber reinforced (FRC) composite components on the mechanical response of model bi-material beams under static loading.

Particular attention was paid to the effects of fiber orientation in the FRC component and spatial arrangement of the strengthening FRC component in the PFC component with respect to the type of loading geometry.

Furthermore, the effect of fiber orientation in the FRC component, the composition of PFC component and the cure protocol on the shear adhesion strength between the two components was investigated.

## 4 EXPERIMENTAL

### 4.1 MATERIALS USED

#### 4.1.1 Fiber reinforced composites (FRC)

Two types of FRC's were used for specimens preparation supplied by *ADM, a.s., Czech Republic*. The first one was a flat strip (PFU) made from S2-glass with unidirectional orientation of fibers and the second one was flat strip made from E-glass fibers (PFM) with multidirectional orientation of fibers. Both strips were preimpregnated by manufacturer with light curing resin based on dimethacrylates.

Supplemental characteristics of FRC strips is in Tab. 2:

*Table 2: Fiber characteristics of FRC strips.*

<b>FRC</b>	<b>Type of glass fibers</b>	<b>Number of fibers</b>	<b>diameter of the fibers (<math>\mu\text{m}</math>)</b>	<b>TEX</b>
PFU	S2-glass	8.400	5	1320
PFM	E-glass	10.700	9	1770

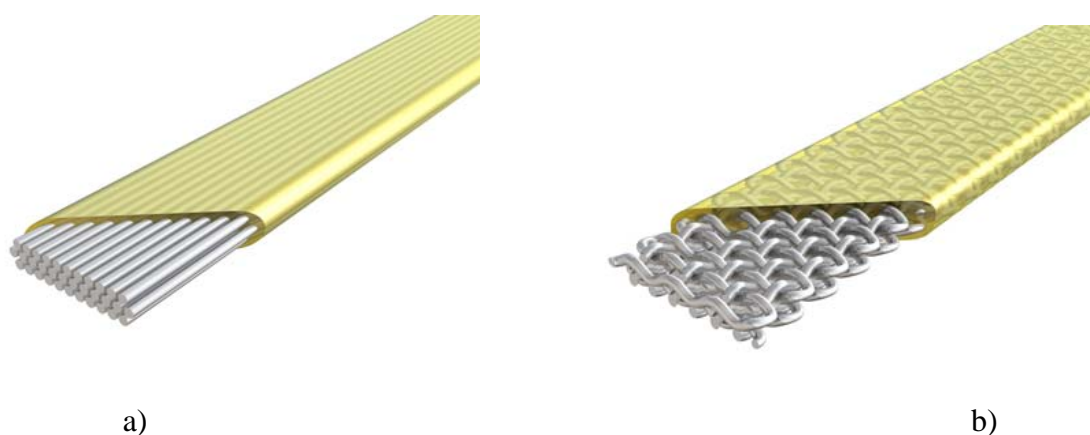


*Figure 12: Structure of PFU (a) and PFM (b) strips.*

### 4.1.2 Particulate composites (PFC)

Two types of particulate composites were used for specimens preparation for shear bond strength tests. The first one was *GC Gradia Direct Flo* (*GC, Japan*), composite of low viscosity. The second one was *Boston* (*Arkona - Laboratorium Farmakologii Stomatologicznej, Poland*), standard Crown&Bridge (C&B) composite. Only Boston PFC was used for 3 and 4-point bending tests.

*Adper Single Bond 2* (*3M ESPE, USA*) adhesive was used for shear bond strength test with interlayer.

**Table 3:** Characteristics of PFC's used.

<b>PFC</b>	<b>Type of material</b>	<b>Content of inorganic particles (wt.%)</b>	<b>Standard deviation (%)</b>
Gradia Direct Flo	flowable	60	1
Boston	C&B	78	1
Adper Single Bond 2	adhesive	0	0

## 4.2 METHODS

### 4.2.1 Thermogravimetric analysis

Thermogravimetric analysis (TGA) is a technique which enables to measure the weight loss of the sample in a specific atmosphere (usually air or nitrogen) as a function of temperature.

A *Perkin Elmer TGA 6 (Perkin Elmer)* instrument was used for measurement of specimens analyzed in this work. Nitrogen atmosphere was selected. Samples of composites (10-15 mg) were heated from 50°C (equilibrated for 1 min) at a heating rate of 10°C/min to 550°C and held for 10 min at this temperature.

### 4.2.2 Shear bond strength tests

Measurements of shear bond strength were carried out using *Universal Testing Machine Zwick Z010 (Zwick, Germany)*. A special steel die was used to mount the specimen. Crosshead speed of 1 mm/min was used in all measurements.

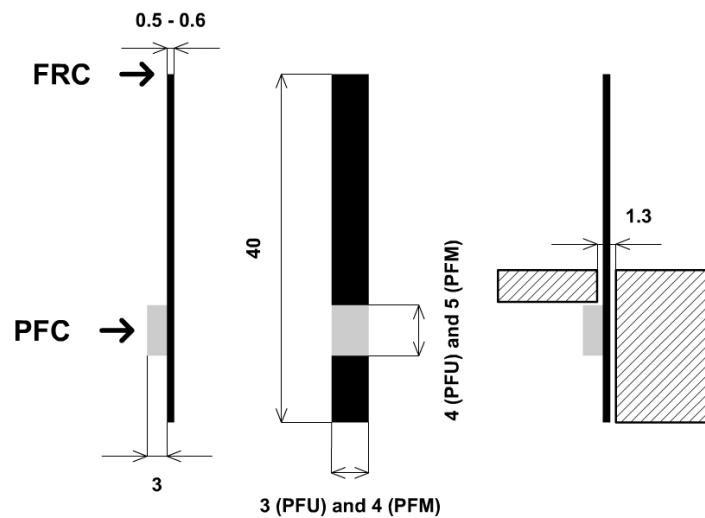


*Figure 13: Scheme showing specimen and bond strength test geometry setup.*

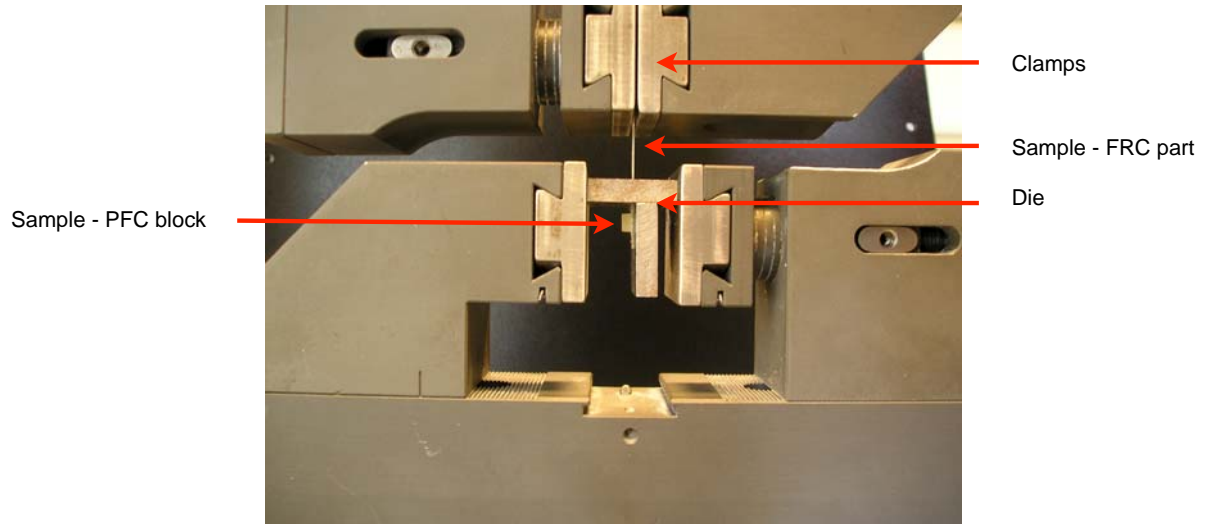


**Figure 14:** Adhesion test arrangement.

The adhesion strength  $\tau_A$  was calculated from the following equation:

$$\tau_A = \frac{F}{S_A \cdot S_B} \quad (17)$$

where:

F = loading force (N)

$S_A$  = height of PFC block (m)

$S_B$  = width of PFC block (m)

### 4.2.3 3-point bending tests

3-point bending tests were carried out using *Universal Testing Machine Zwick Z010* (Zwick, Germany). Crosshead speed of 2 mm/min was used in all measurements. The length of the specimens were 40 mm. The support span was 30 mm.

The flexural stress  $\sigma_f$  was calculated from the following equation:

$$\sigma_f = \frac{3 \cdot F \cdot L}{2 \cdot b \cdot h} \quad (18)$$

where:

F = loading force (N)

L = support span (mm)

b = width of the specimen

h = depth of the specimen

For simplification, the modulus of elasticity was calculated as for isotropic homogeneous material. Young's modulus  $E_C$  was calculated as an angular coefficient of functional relation of flexural stress on relative deformation. The selected range for calculation was from  $5 \cdot 10^{-4}$  to  $25 \cdot 10^{-4}$  of relative deformation according to ČSN EN ISO 178. In reality,  $E_C$  is an average value of Young's moduli of individual components of bi-material specimens.

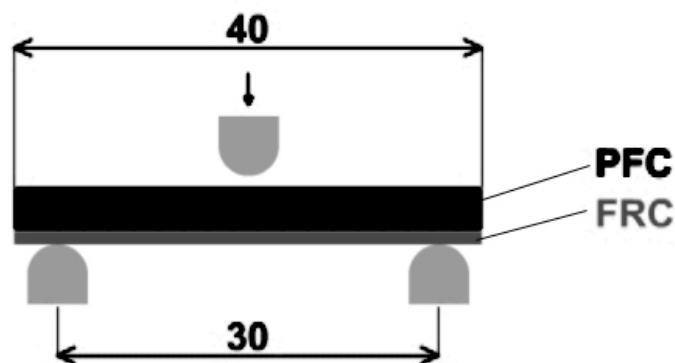


*Figure 15: Scheme showing 3-point bending test geometry setup.*

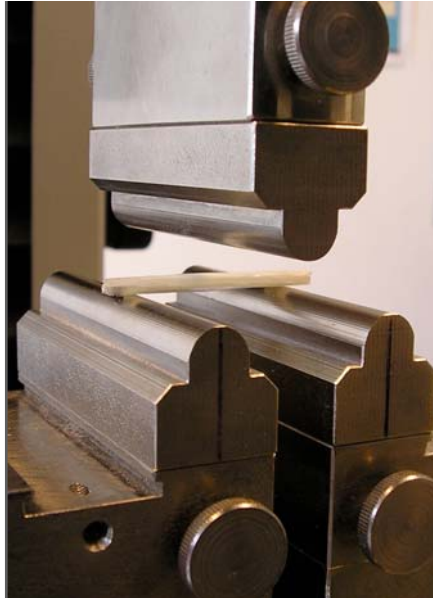


**Figure 16:** 3-point bending tests arrangement.

#### **4.2.4 4-point bending tests**

4-point bending tests were carried out using *Universal Testing Machine Zwick Z010* (Zwick, Germany). Crosshead speed of 2 mm/min was used in all measurements. The length of the specimens were 40 mm. The support span was 30 mm and the load span was 16 mm.

The flexural stress  $\sigma_f$  was calculated from the following equation:

$$\sigma_f = \frac{3 \cdot F \cdot L}{4 \cdot b \cdot h^2} \quad (19)$$

where:

F = loading force (N)

L = support span (mm)

b = width of the specimen

h = depth of the specimen

For simplification, the modulus of elasticity was calculated as for isotropic homogeneous material. Young's modulus  $E_C$  was calculated as an angular coefficient of functional relation of flexural stress on relative deformation. The selected range for calculation was from  $5 \cdot 10^{-4}$  to  $25 \cdot 10^{-4}$  of relative deformation according to ASTM-D 6272. In reality,  $E_C$  is an average value of Young's moduli of individual components of bi-material specimens.

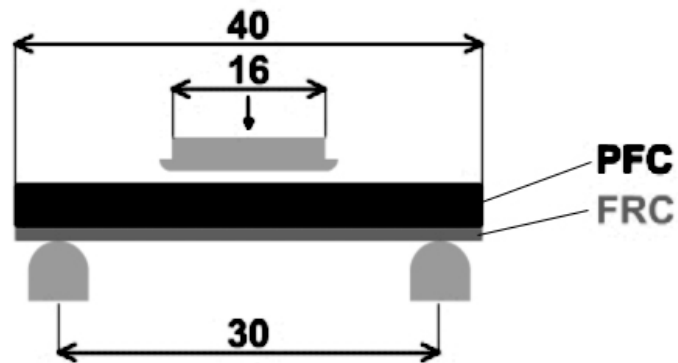


*Figure 17: Scheme showing 4-point bending test geometry setup.*

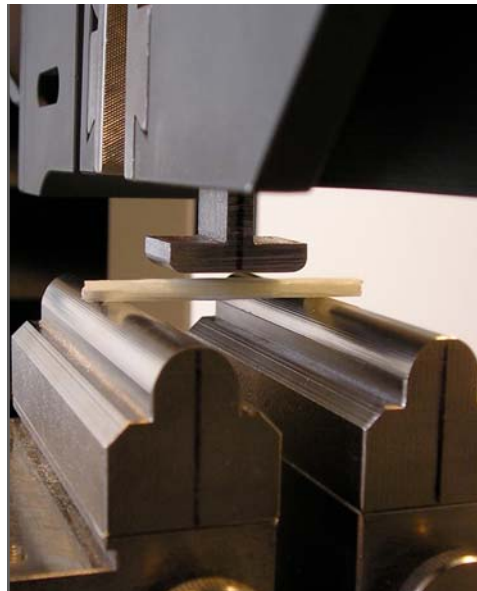


*Figure 18: 4-point bending tests arrangement.*

#### **4.2.5 Scanning Electron Microscopy**

The scanning electron microscope (SEM) *Philips 30 (Philips)* was used to observe crack surface of specimens. Fracture surfaces were coated with Au before placing into the SEM chamber.

## 4.3 SPECIMEN PREPARATION

### 4.3.1 Shear bond strength tests

FRC strip was placed into the transparent rubber mold *Lukopren* with rectangular cavity. Then it was flattened with the block of rubber and light polymerized in light curing chamber *Targis Power* (*Ivoclar, Liechtenstein*) for 5 minutes. For specimens with interlayer (*Adper Single Bond 2*) a thin layer of bond was placed on light cured FRC and light cured for 2 minutes. Another rubber mold was used to build up the PFC substrate. This mold consisted of two rectangular cavities. The FRC strip was placed into the larger one, whereas the PFC block was prepared in the smaller one. Such prepared specimen was light cured in light curing chamber for another 5 minutes. In the case that whole specimen (FRC and PFC) was cured at once the whole structure was cured for 10 minutes. Five specimens were prepared for each type of measurement. Schedule of specimen preparation is shown in Table 4.

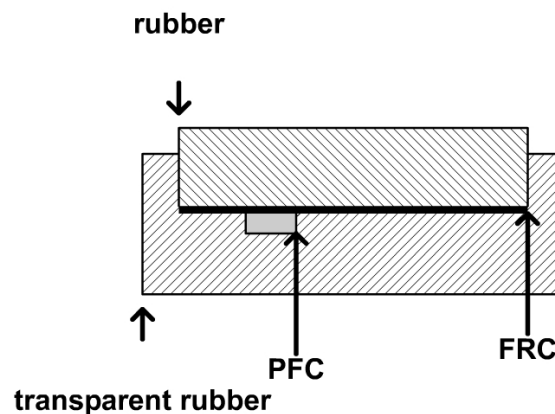


*Figure 19: Scheme showing specimen preparation.*



*Figure 20: Shear bond strength - specimen preparation.*

**Table 4:** Schedule of specimen preparation.

Type of specimen	Schedule
no interlayer, FRC cured first	Schedule A
no interlayer, cured at once	Schedule B
with interlayer, FRC cured first	Schedule C

### 4.3.2 3 and 4-point bending tests

FRC strip was placed into the transparent rubber mold *Lukopren* with rectangular cavity. The dimensions of the cavity were 40 x 3 x 2 mm (length x width x depth). For specimens with FRC neither at the bottom or at the top was the strip placed in the cavity, covered with PFC and light polymerized in light curing chamber *Targis Power (Ivoclar, Liechtenstein)* for 10 minutes. For specimens with FRC in the middle, just one half of the PFC was put inside the cavity. Then the strip was put inside and covered with the rest of PFC. FRC strip was cured for 1 minute for the samples where the FRC was cured first before placing in PFC. Five specimens were prepared for each type of measurement. Schedule of specimen preparation is shown in Table 5.



**Fig 21:** Specimens preparation for 3 and 4-point bending tests.

**Table 5:** Schedule of specimen preparation, PFU/Boston.

<b>Type of specimen</b>	<b>Schedule</b>
FRC in the upper part, FRC cured first	Schedule D
FRC in the middle part, FRC cured first	Schedule E
FRC in the bottom part, FRC cured first	Schedule F
FRC in the bottom part, cured at once	Schedule G

## 5 RESULTS AND DISCUSSION

### 5.1 STRUCTURAL ANALYSIS OF THE FRC

Thermogravimetric analysis was used for determination of fibers weight content  $w_f$  (%) in unidirectional and multidirectional FRC composites. It was shown that with increasing temperature up to 400°C the weight content (%) of the resin was decreasing linearly. In the range from 400 to 450°C the decreasing of resin weight content is not so steep, however from 450°C to 500°C the decreasing of resin weight content continuous linearly up to 500°C where no next change is apparent (Fig. 23). From this dependence it is assumed that resin in both PFM and PFU composites is a mixture of the monomers which are decomposed in different temperature according to TGA diagrams. From the TGA data it was calculated that multidirectionally oriented woven FRC composites (PFM) contain  $55 \pm 3$  wt.% of fibers and unidirectionally oriented composites (PFU) contain  $60 \pm 3$  wt.% of fibers, respectively (Fig. 22, 23).

These results are in a good agreement with manufacturer data and signalize that lower fibers weight fraction in PFM composites in combination with smaller fibers diameter (approx.  $9 \mu\text{m}$ ), which was determinate from SEM measurements (Fig. 24) compared to PFU with fibers diameter (approx.  $5 \mu\text{m}$ ) (Fig. 25), ensure higher flexibility of the composite. On the other hand, it is assumed that the mechanical properties of these composites, especially Young's modulus ( $E_C$ ) and ultimate strength ( $\sigma_U$ ), are lower than these of unidirectional ones. The mechanical properties of FRC composites are discussed more detailed in section 5.2.

**Table 6:** Fiber content and fiber orientation of PFM and PFU composites.

Type of FRC	Fiber content (wt.%)	Fiber orientation
<b>PFM</b>	$55 \pm 3.0$	multidirectional
<b>PFU</b>	$60 \pm 3.0$	unidirectional

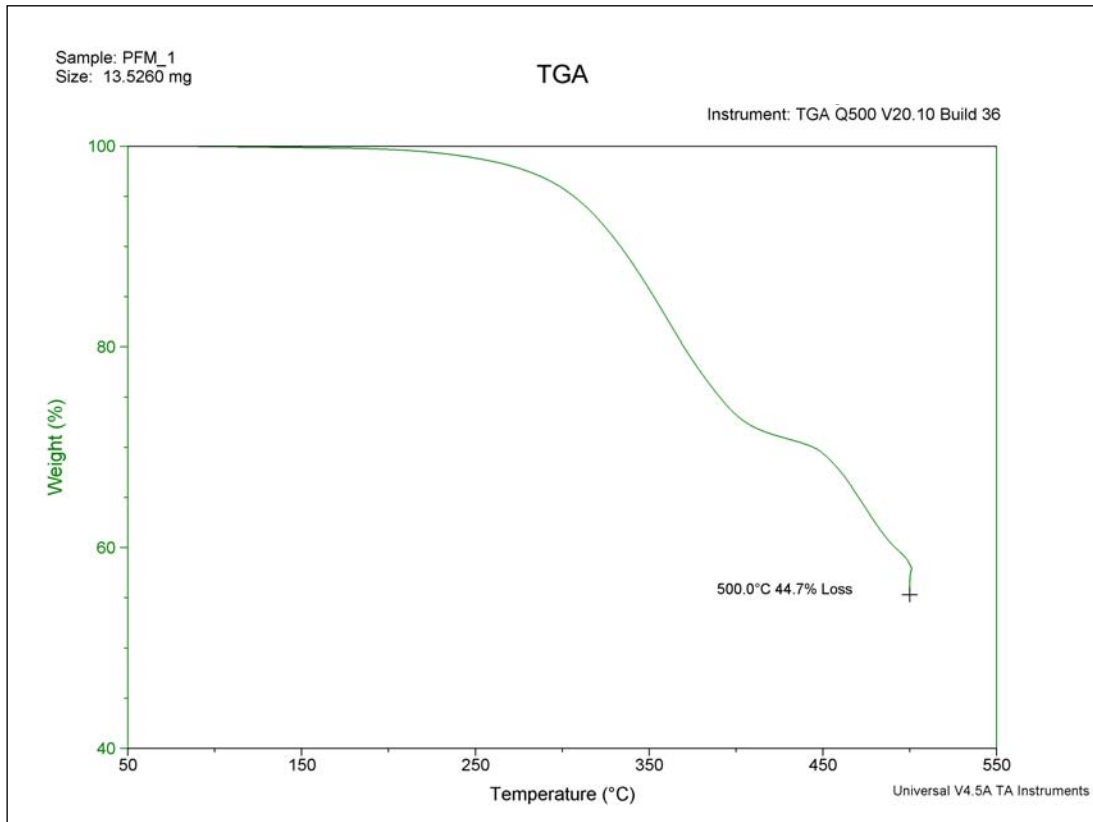


Figure 22: Sample of fiber weight fibers content (%) vs. temperature  $T$  (°C) dependence for PFM strip.

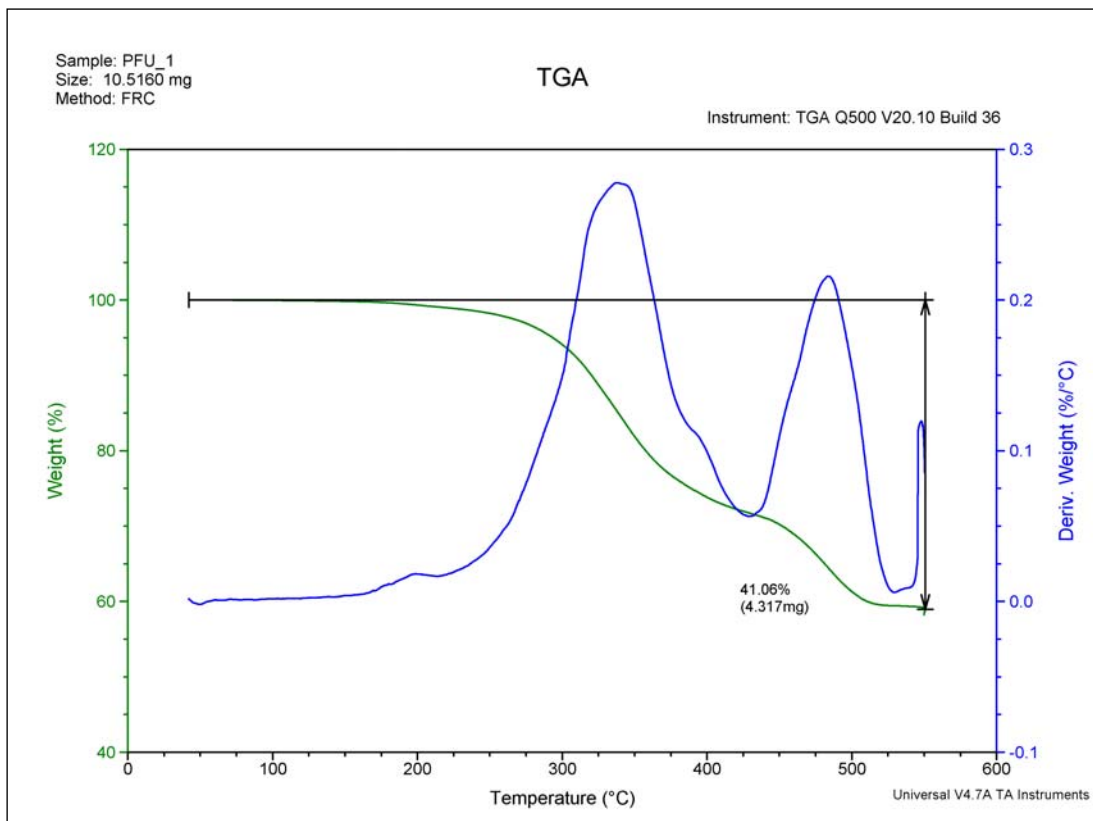
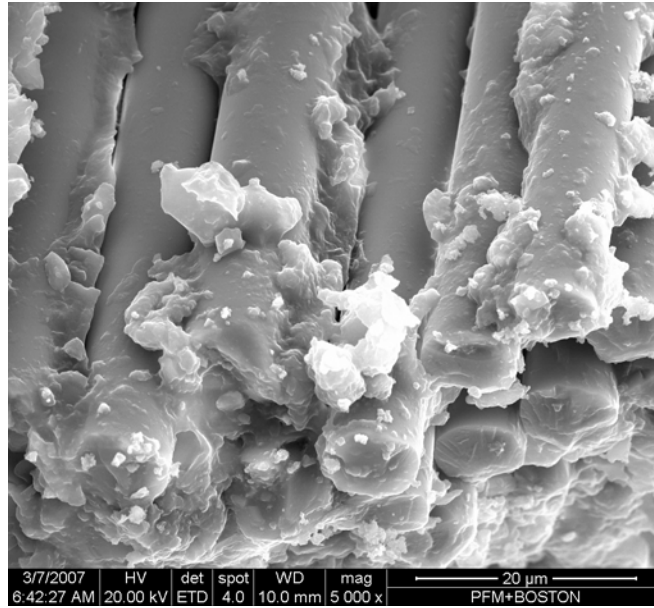
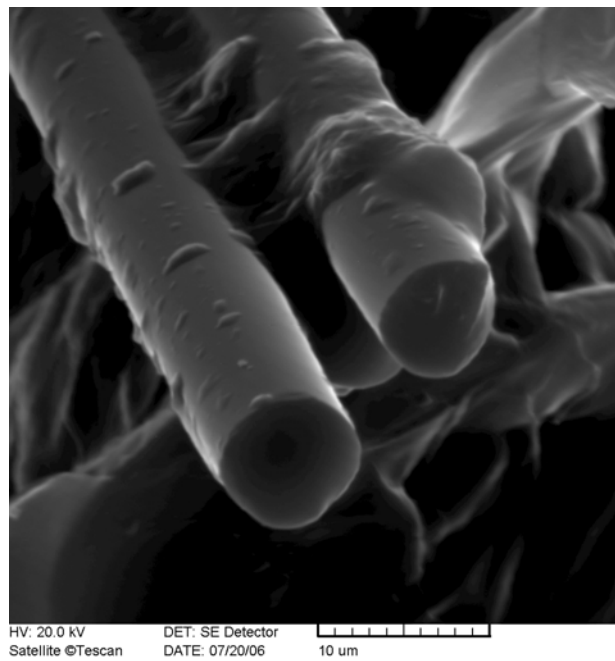


Figure 23: Sample of fiber weight fibers content (%) vs. temperature  $T$  (°C) dependence for PFM strip.



*Figure 24: SEM photography (at 5000 magnification) showing the diameter of the fibers in PFM strip.*



*Figure 25: SEM photography (at 10000 magnification) showing the diameter of the fibers in PFU strip.*

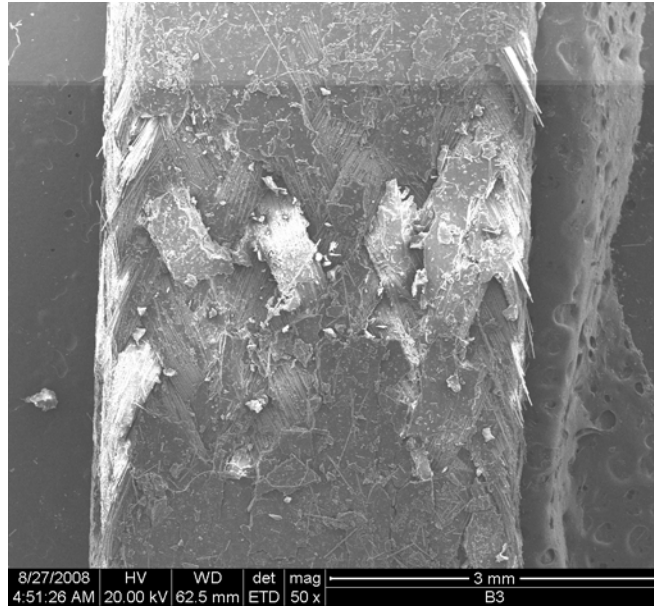


*Figure 26: SEM photography (at 50 magnification) showing the structure of PFM strip.*

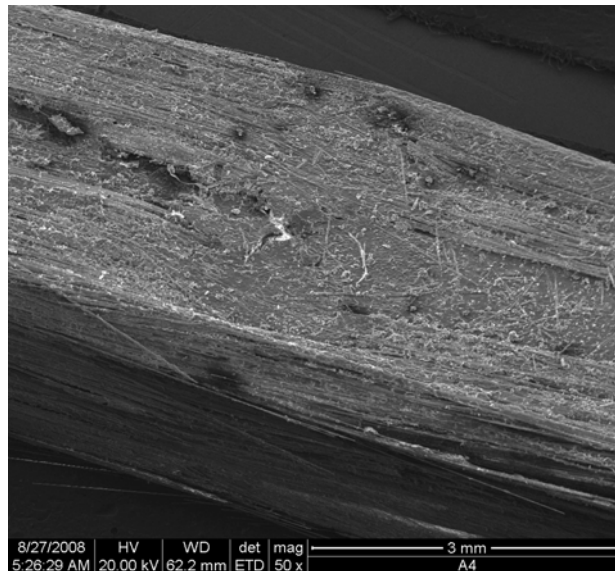


*Figure 27: SEM photography (at 50 magnification) showing the structure of PFU strip.*

## 5.2 MECHANICAL PROPERTIES OF COMPOSITES

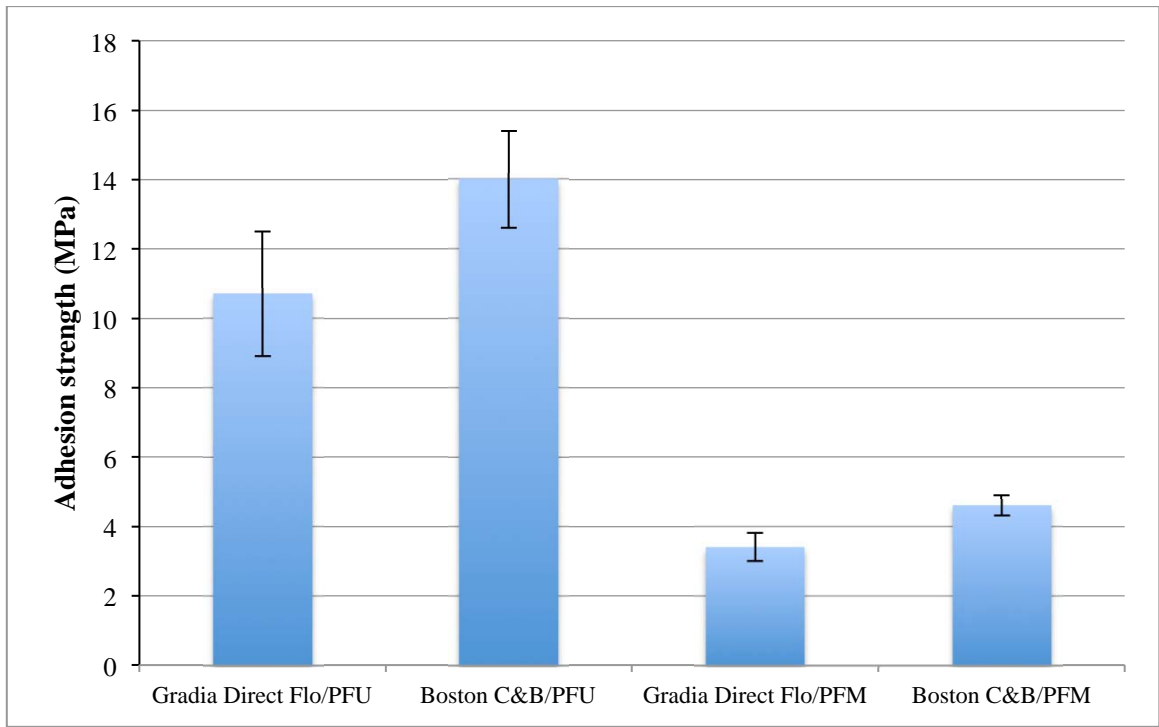
### 5.2.1 Shear adhesion strength

#### 5.2.1.1 Samples prepared according schedule A

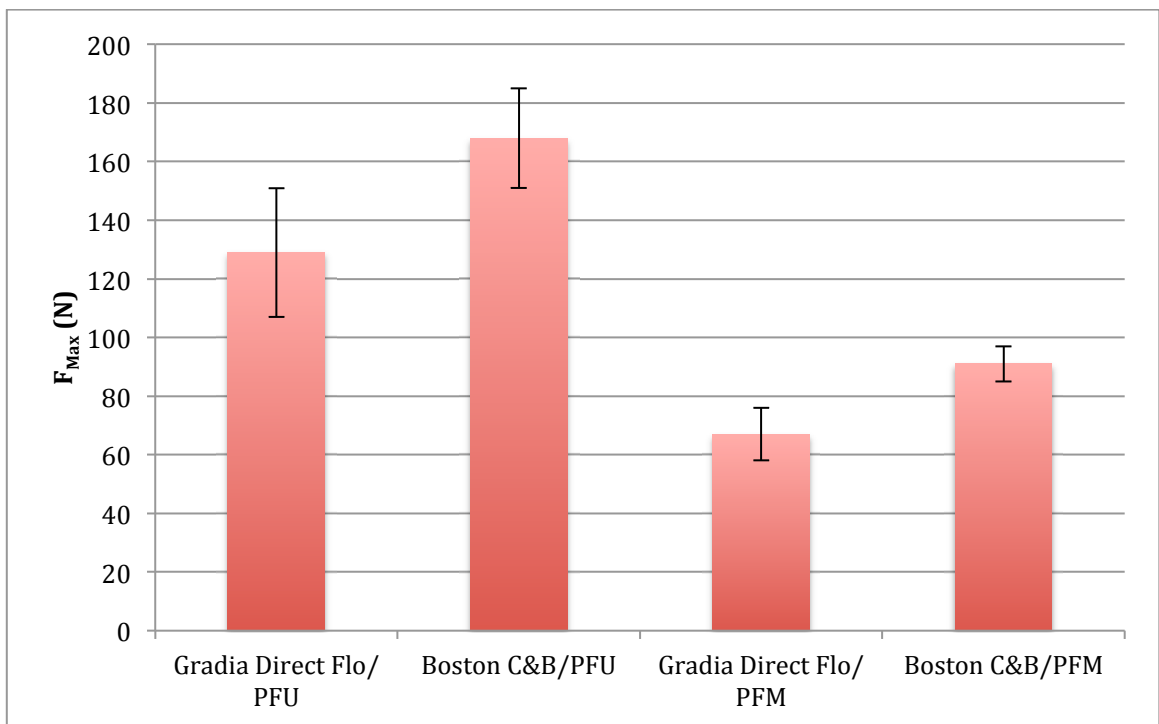
The effect of different methods of FRC and PFC composites preparation without interlayer, especially type of light curing, on strength in adhesion  $\tau_A$  was characterized utilizing modified pull-out test. Four groups of FRC and PFC materials were tested and  $\tau_A$  was calculated according to Eq. 17. In Fig. 28 it is apparent that adhesion strength  $\tau_A$  is increasing in the row PFM + Gradia Flo, PFM + Boston C&B, PFU + Gradia Flo, PFU + Boston C&B. This trend signalizes that unidirectional oriented FRC composites contribute more substantially to strength in adhesion of FRC + PFC composites than multidirectional oriented ones in spite of their adhesion area is smaller. The failure of the composites starts on interphase between FRC and PFC and continuous to FRC composite. This effect is apparent for unidirectional strips. However, the effect of FRC damage is low, because there is no interlayer which ensures the bond between FRC and PFC (Fig. 29 - 32).

**Table 7:** Strength in adhesion between different FRC and PFC, sample preparation – schedule A.

FRC	PFC	Category of PFC	S <sub>A</sub> height (mm)	S <sub>A</sub> width (mm)	Avg. F <sub>MAX</sub> (N)	Avg. $\tau_A$ (MPa)
PFU	Gradia direct Flo	flow	3	4	129±22	10.7±1.8
PFU	Boston C&B	C&B	3	4	168±17	14.0±1.4
PFM	Gradia direct Flo	flow	4	5	67±9	3.4±0.4
PFM	Boston C&B	C&B	4	5	91±6	4.6±0.3



(a)



(b)

**Figure 28:** Strength in adhesion (a) and maximum force (b) between different FRC and PFC, sample preparation – schedule A.

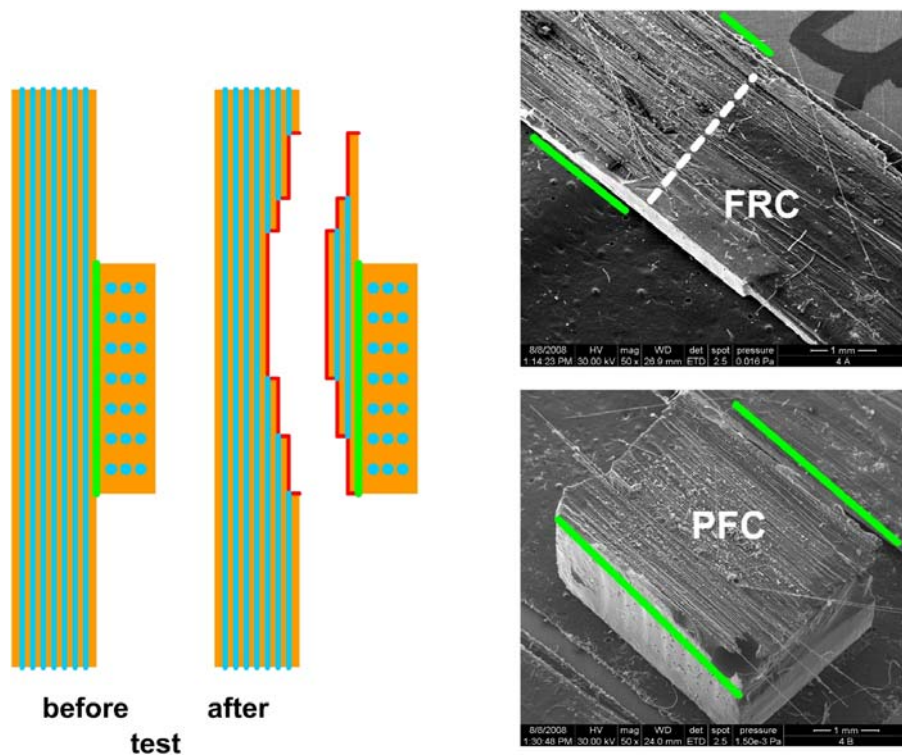


**Figure 29:** SEM photographs and scheme of PFU + Gradia direct Flo composite adhesion surfaces (at 50x magnification) after pull-out test, sample preparation – schedule A.

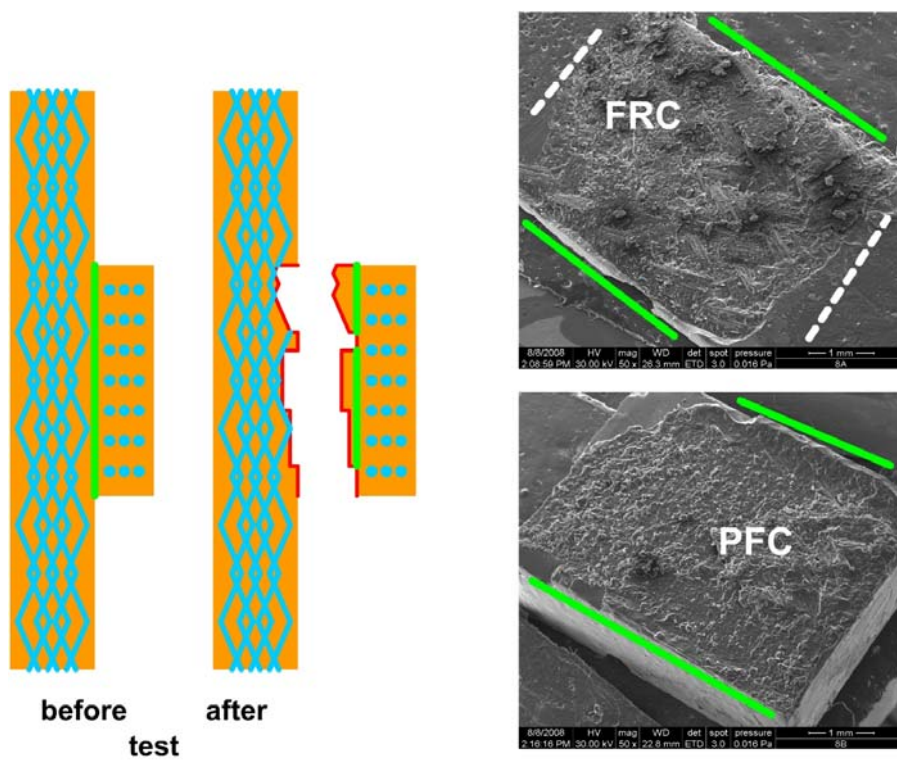


**Figure 30:** SEM photographs and scheme of PFM + Gradia direct Flo composite adhesion surfaces (at 50x magnification) after pull-out test, sample preparation – schedule A.

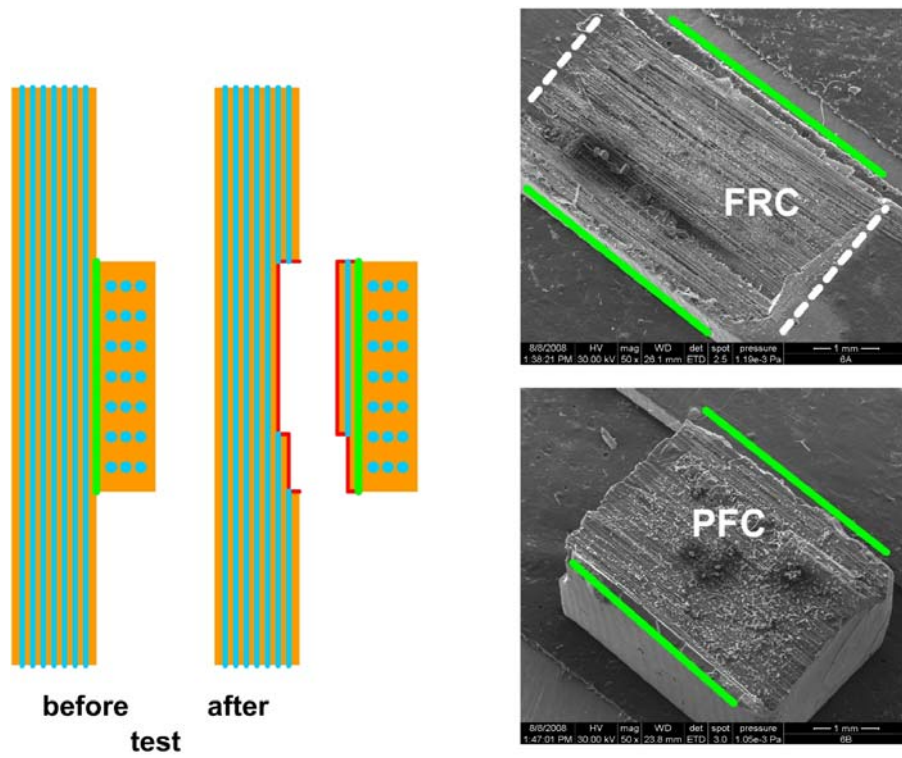


*Figure 31: SEM photographs and scheme of PFU + Boston composite surfaces (at 50x magnification) after pull-out test, sample preparation – schedule A.*

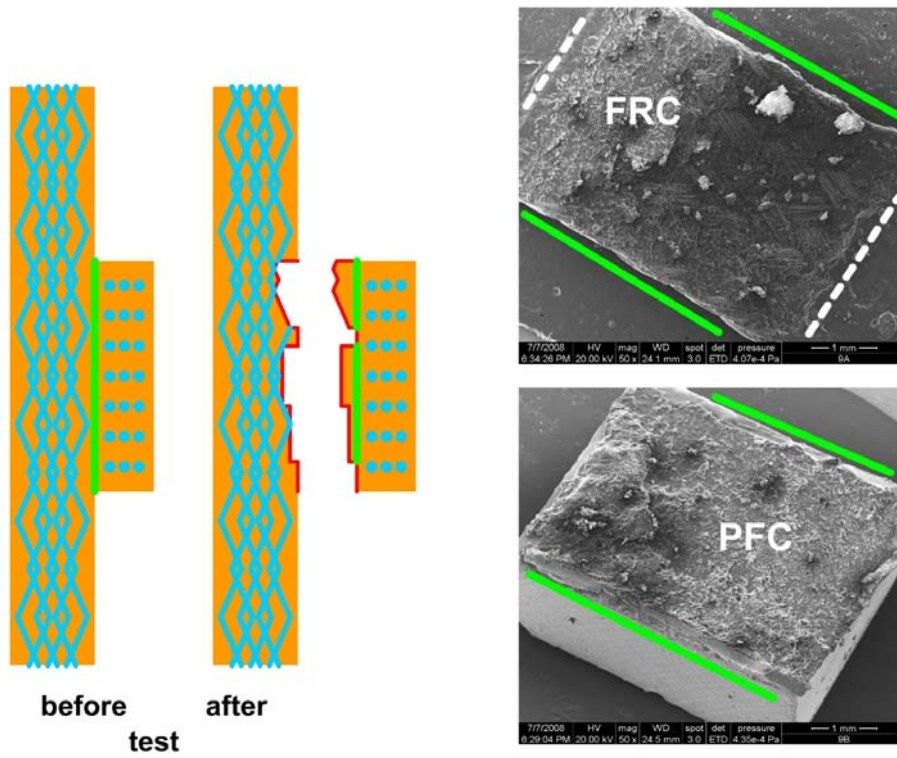


*Figure 32: SEM photographs and scheme of PFM + Boston composite surfaces (at 50x magnification) after pull-out test, sample preparation – schedule A.*

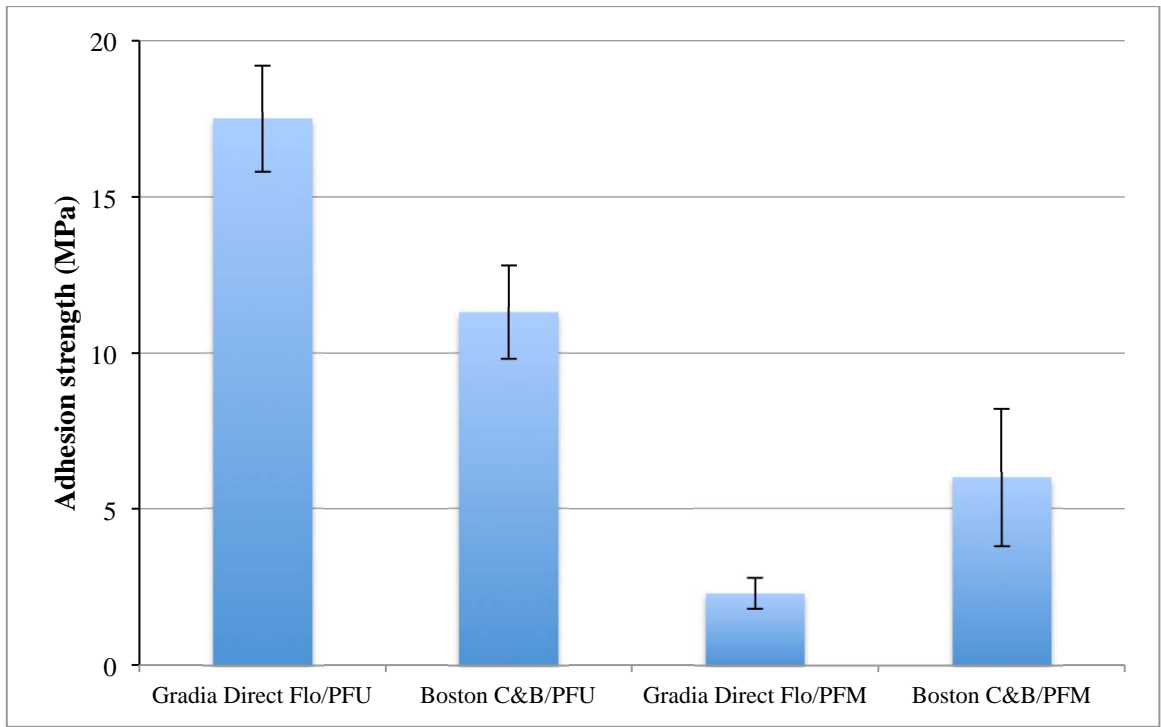
### 5.2.1.2 Samples prepared according schedule B

The second group of hybrid FRC and PFM composites was tested under the same test conditions as the first one. The only one difference was that the samples were light cured at ones, it means, that FRC and PFC were light cured simultaneously. The effect of the way of light curing on strength in adhesion was evaluated utilizing modified pull-out test. The calculated values of the  $\tau_A$  are shown in Table 8.

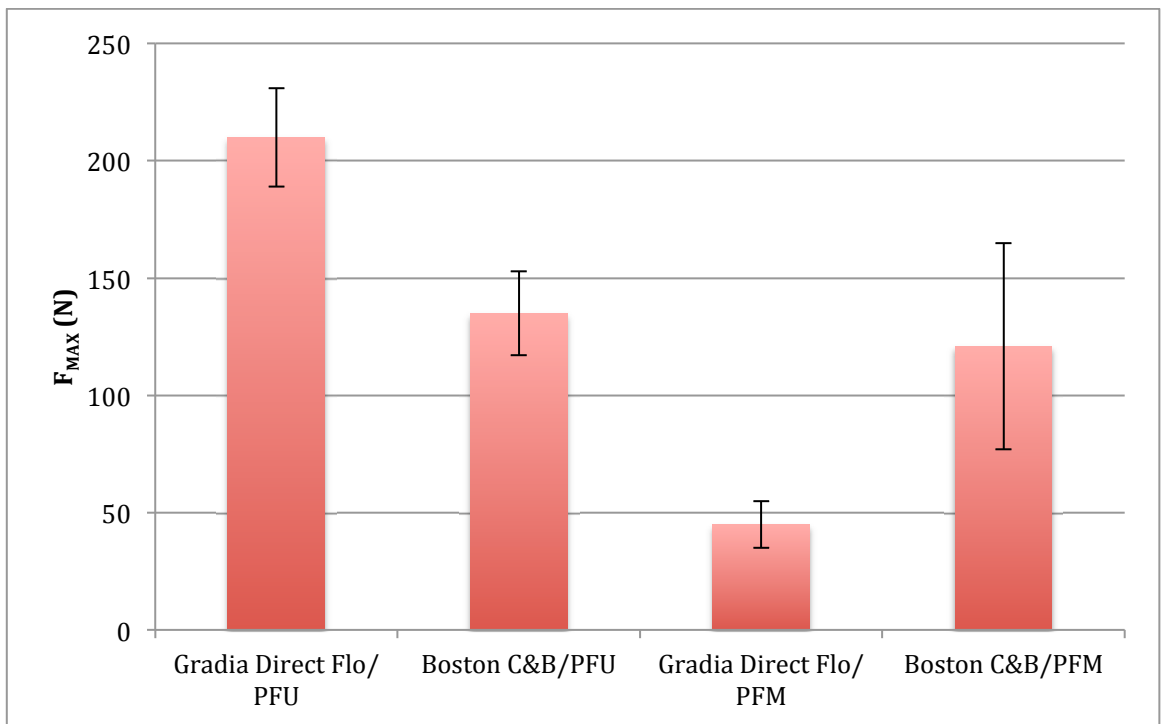
**Table 8:** Strength in adhesion between different FRC and PFC, sample preparation – schedule B.

<b>FRC</b>	<b>PFC</b>	<b>Category of PFC</b>	<b>S<sub>A</sub> height (mm)</b>	<b>S<sub>B</sub> width (mm)</b>	<b>Avg. F<sub>MAX</sub> (N)</b>	<b>Avg. <math>\tau_A</math> (MPa)</b>
PFU	Gradia direct Flo	flow	3	4	210±21	17.5±1.7
PFU	Boston C&B	C&B	3	4	135±18	11.3±1.5
PFM	Gradia direct Flo	flow	4	5	45±10	2.3±0.5
PFM	Boston C&B	C&B	4	5	121±44	6.0±2.2

The failure of the FRC + PFC hybrid composite starts on interphase between FRC and PFC. Then the failure goes through a small layer of FRC against to FRC-PFC interlayer. The effect of the simultaneously light curing is apparent from Fig. 34 where the failure continuous through micro-mechanical interphase into the fibers in FRC composite. This effect contributes to enhance of strength in adhesion of bi-material composites cured at once in contrast to bi-material composites, where FRC was cured at first. Moreover, bi-material composites with unidirectional oriented FRC where the fibers are oriented in pull-out direction exhibit higher values of strength in adhesion than multidirectional ones.



(a)



(b)

**Figure 33:** Strength in adhesion (a) and maximum force (b) between different FRC and PFC, sample preparation – schedule B.

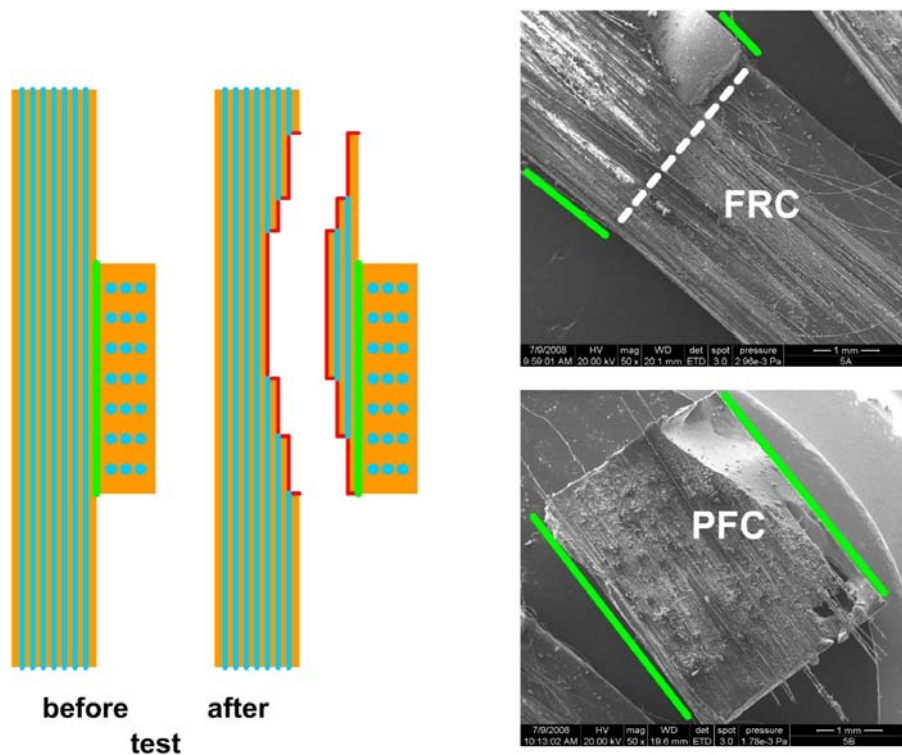


**Figure 34:** SEM photographs and scheme of PFU + Gradia direct Flo composite adhesion surfaces (at 50x magnification) after pull-out test, sample preparation – schedule B.

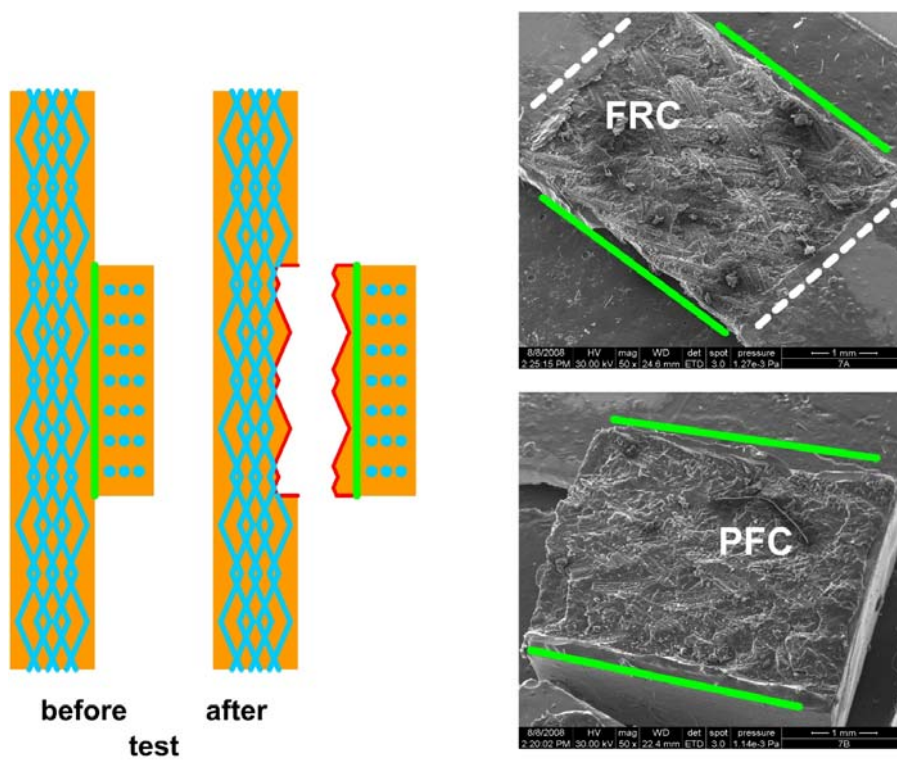


**Figure 35:** SEM photographs and scheme of PFM + Gradia direct Flo composite adhesion surfaces (at 50x magnification) after pull-out test, sample preparation – schedule B.

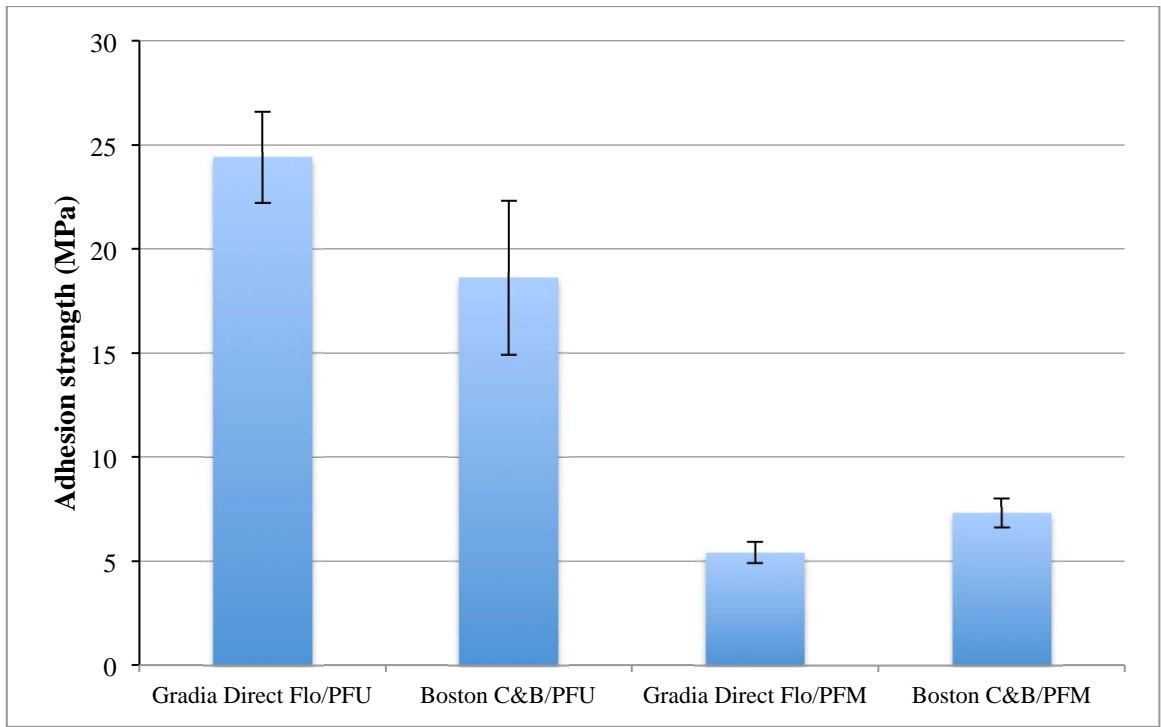
### 5.2.1.3 Samples prepared according schedule C

To enhance the strength in adhesion of FRC + PFC composites, adhesive (Adapter Single Bond 2) was added between FRC and PFC composite layer. The samples were prepared and tested according to 5.2.1.1, where FRC was light cured at first. The results of modified pull-out tests are shown in Table 9.

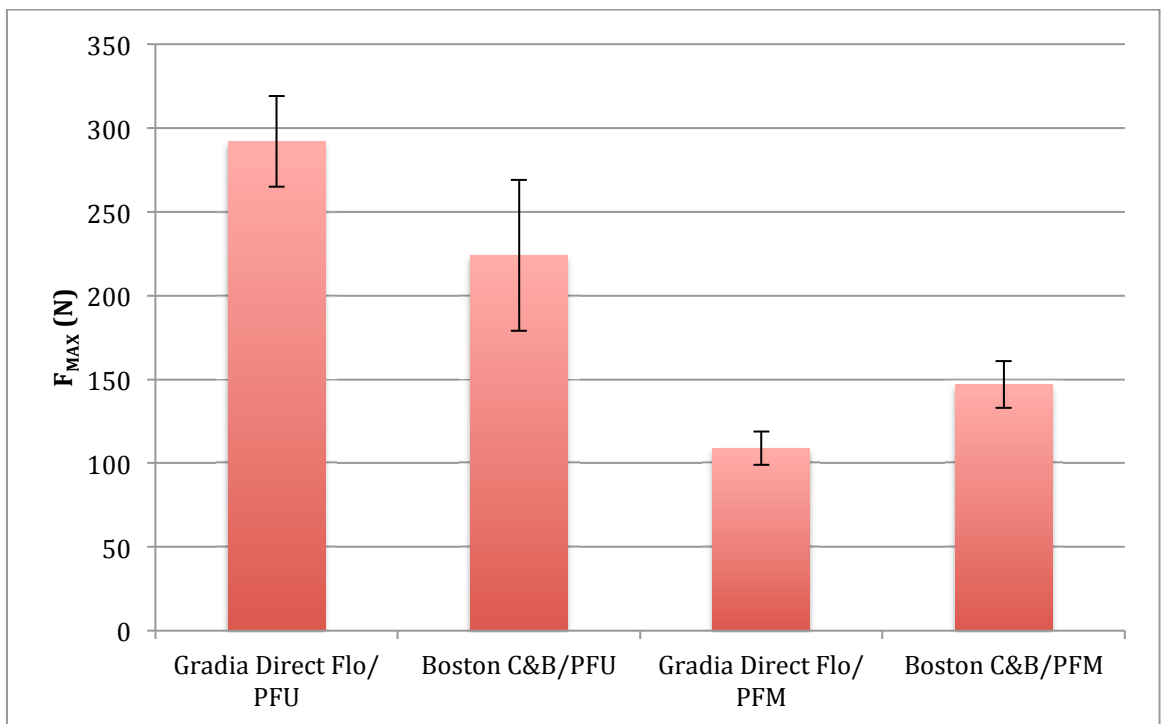
**Table 9:** Strength in adhesion between different FRC and PFC, sample preparation – schedule C.

<b>FRC</b>	<b>PFC</b>	<b>Category of PFC</b>	<b>S<sub>A</sub> height (mm)</b>	<b>S<sub>B</sub> width (mm)</b>	<b>Avg. F<sub>MAX</sub> (N)</b>	<b>Avg. τ<sub>A</sub> (MPa)</b>
PFU	Gradia direct Flo	flow	3	4	292±27	24.4±2.2
PFU	Boston C&B	C&B	3	4	224±45	18.6±3.7
PFM	Gradia direct Flo	flow	4	5	109±10	5.4±0.5
PFM	Boston C&B	C&B	4	5	147±14	7.3±0.7

The failure of the FRC + PFC hybrid composite starts on interphase between FRC and PFC. Then the failure goes through FRC strip. The effect of the adhesive layer is apparent from Fig. 37. This effect contributes to significant enhance of strength in adhesion of bi-material composites with adhesive layer in contrast to bi-material composites without it.



(a)



(b)

**Figure 36:** Strength in adhesion (a) and maximum force (b) between different FRC and PFC, sample preparation – schedule C.

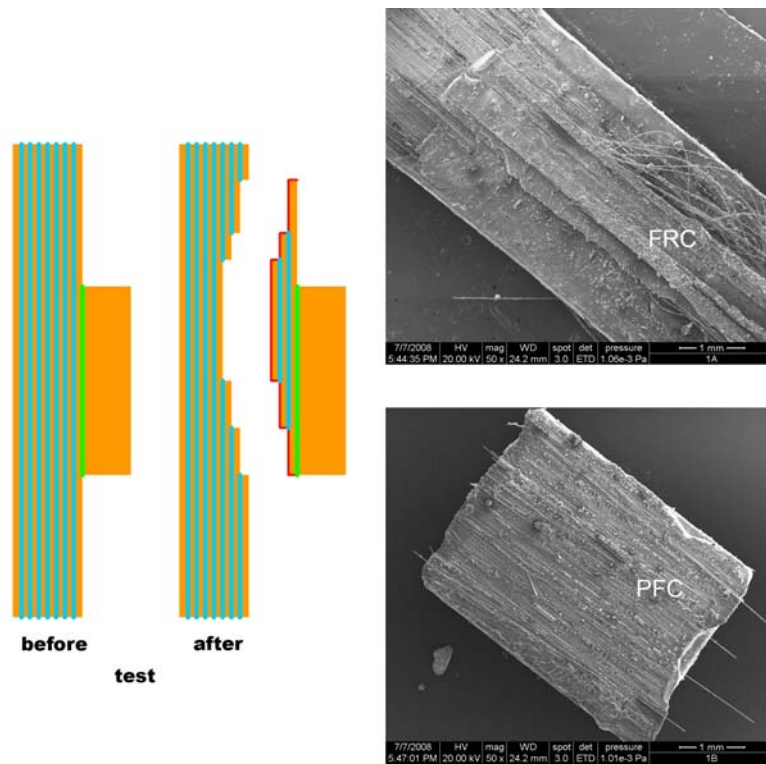


**Figure 37:** SEM photographs and scheme of PFU + Gradiadirect Flo composite adhesion surfaces (at 50x magnification) after pull-out test, sample preparation – schedule C.

## 5.2.2 Young's modulus and ultimate strength in 3-point bending test

Three point bending tests were carried out to calculate Young's modulus ( $E_C$ ) and ultimate strength ( $\sigma_U$ ) of PFU and C&B dental composites with different PFU position according to (eq. 18).

### 5.2.2.1 Properties of components

It is apparent that with increasing fiber weight content and parallel fibers orientation the  $E_C$  and  $\sigma_U$  are also increasing (Table 10). It is in a good agreement with the results from TGA analysis and SEM observations (Table 6, Fig. 24, 25).

**Table 10:** Young's modulus and ultimate strength of PFM and PFU composites.

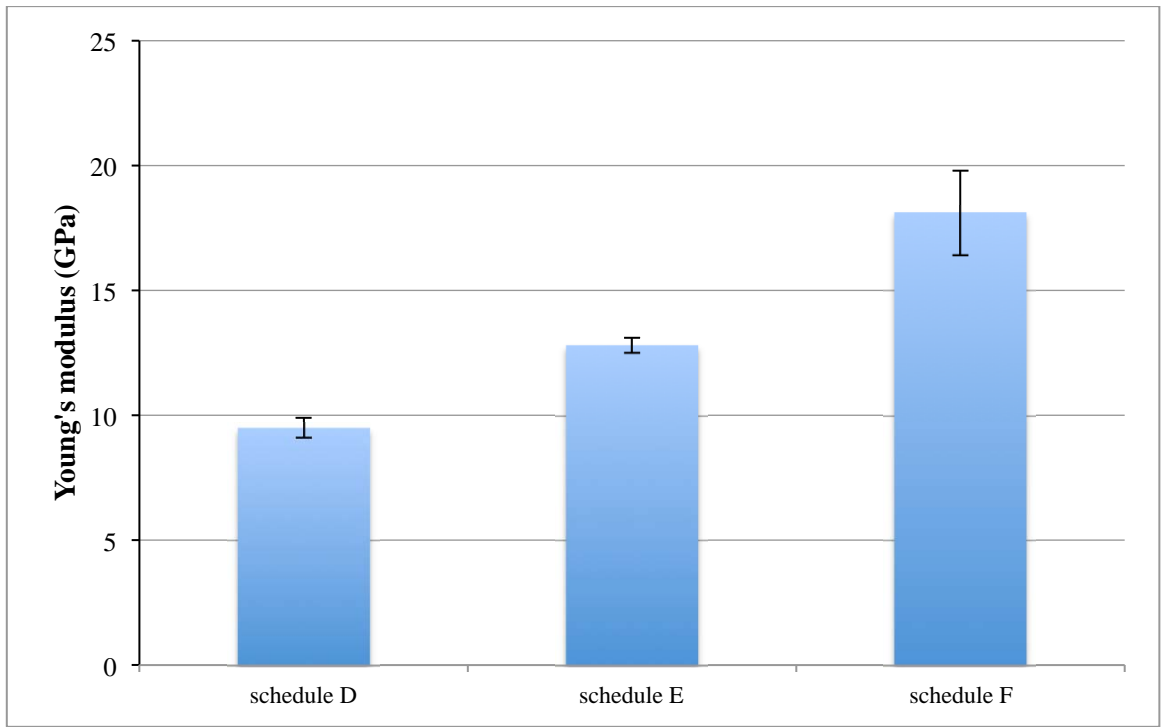
Component	Young's modulus (GPa)	Ultimate strength (MPa)
<b>PFU</b>	29.2 ± 1.9	700 ± 90
<b>PFM</b>	11.7 ± 1.0	160 ± 10
<b>Boston C&amp;B</b>	10.8 ± 0.6	140 ± 10
<b>Gradia Direct Flo</b>	7 ± 0.4	90 ± 10

### 5.2.2.2 C&B composite reinforced with FRC in different position

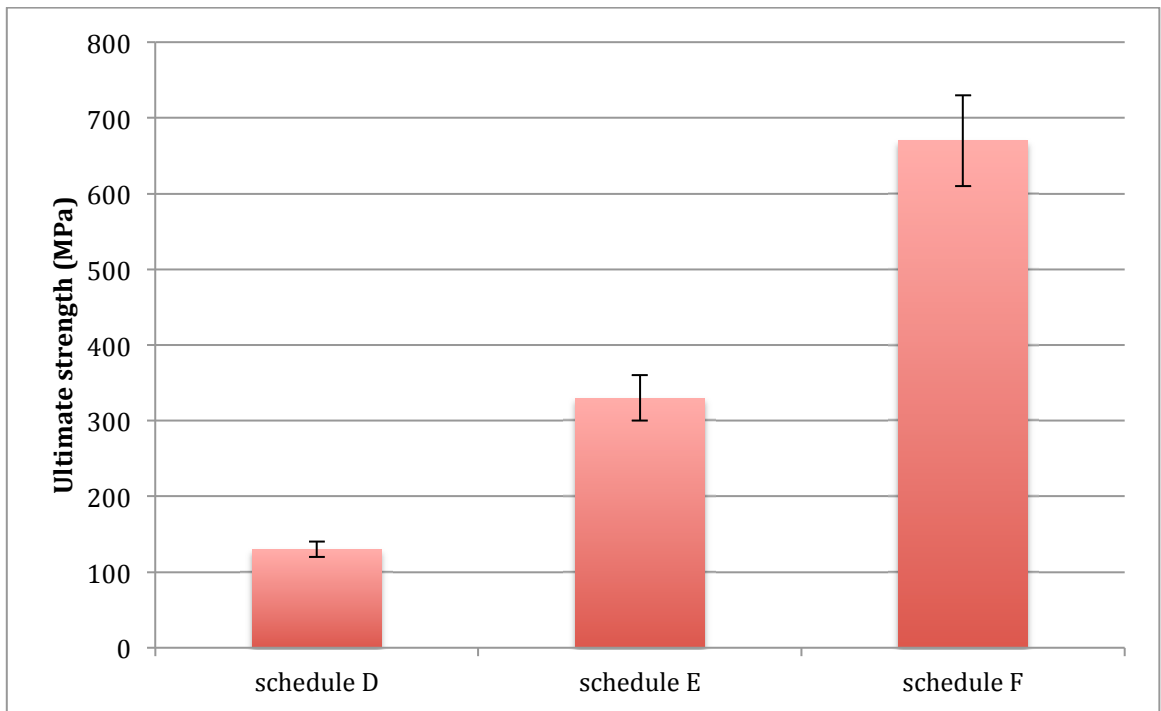
The effect of the position of the PFU strip embedded in C&B composite on mechanical properties of PFC composite was studied utilizing three point bending test. PFU strip was placed in the upper part of C&B, in the middle and in the bottom of C&B composite, respectively. PFU strip was cured first and then was placed to required place in C&B composite, cover with another layer of C&B composite and finally the whole structure was light cured. Effect of the FRC position in PFC is apparent from Fig. 38.

**Table 11:** Young's modulus and ultimate strength of PFU/C&B composites with different position of PFU.

PFU/C&B composite (Arkona)	Young's modulus (GPa)	Ultimate strength (MPa)
sample preparation-schedule D	9.5 ± 0.4	130 ± 10
sample preparation-schedule E	12.8 ± 0.3	330 ± 30
sample preparation-schedule F	18.1 ± 1.7	670 ± 60



(a)



(b)

**Figure 38:** Effect of FRC position on Young's modulus (a) and ultimate strength (b) of PFU/C&B composites.

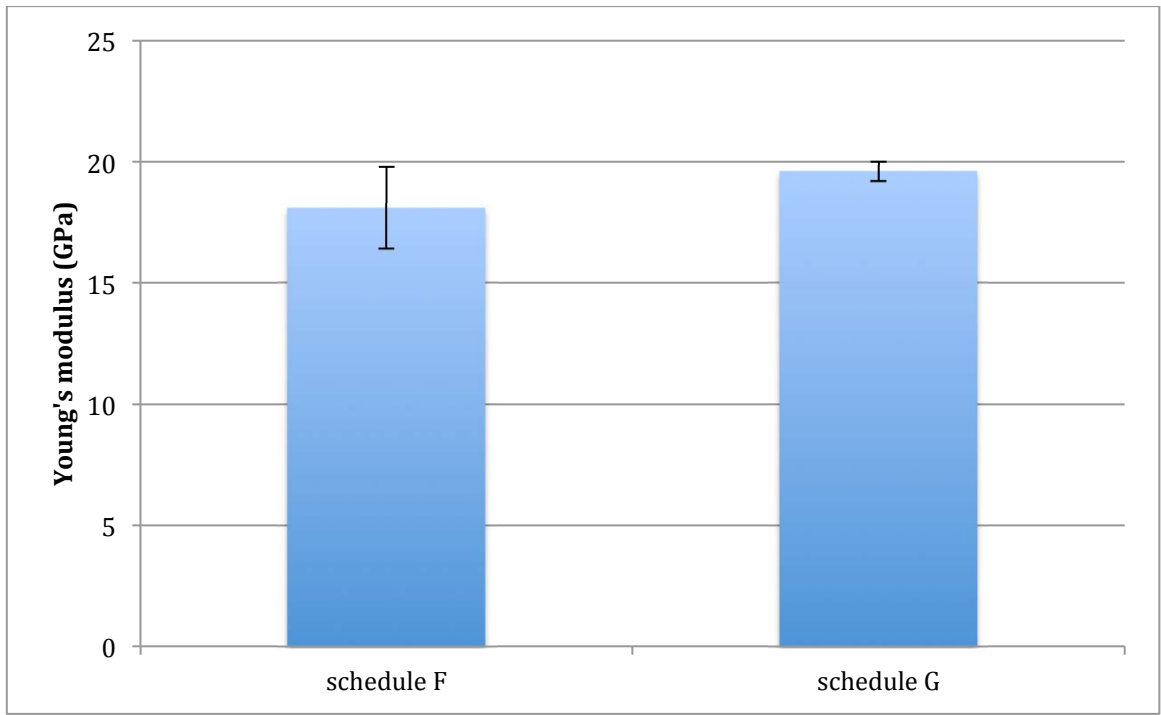
Young's modulus and ultimate strength of FRC/PFC composite are increasing with decreasing position of FRC in PFC composites. During the 3-point bending test is the bottom part of the sample loaded in tension while the upper part of C&B reinforced with FRC is loaded in compression. C&B particle composite is resistant to loading in compression, however in tension is its resistance very restricted. Instead of PFC, FRC is resistant against tensile loading. From this reason, the reinforcing effect of FRC in the bottom part of PFC where the highest tension occurs is the most evident. These results are in a good agreement with the theory [1]. Like as position of FRC in PFC, the effect of FRC/PFC adhesion on mechanical properties of composite is also important.

### 5.2.2.3 C&B composite reinforced with FRC at the bottom

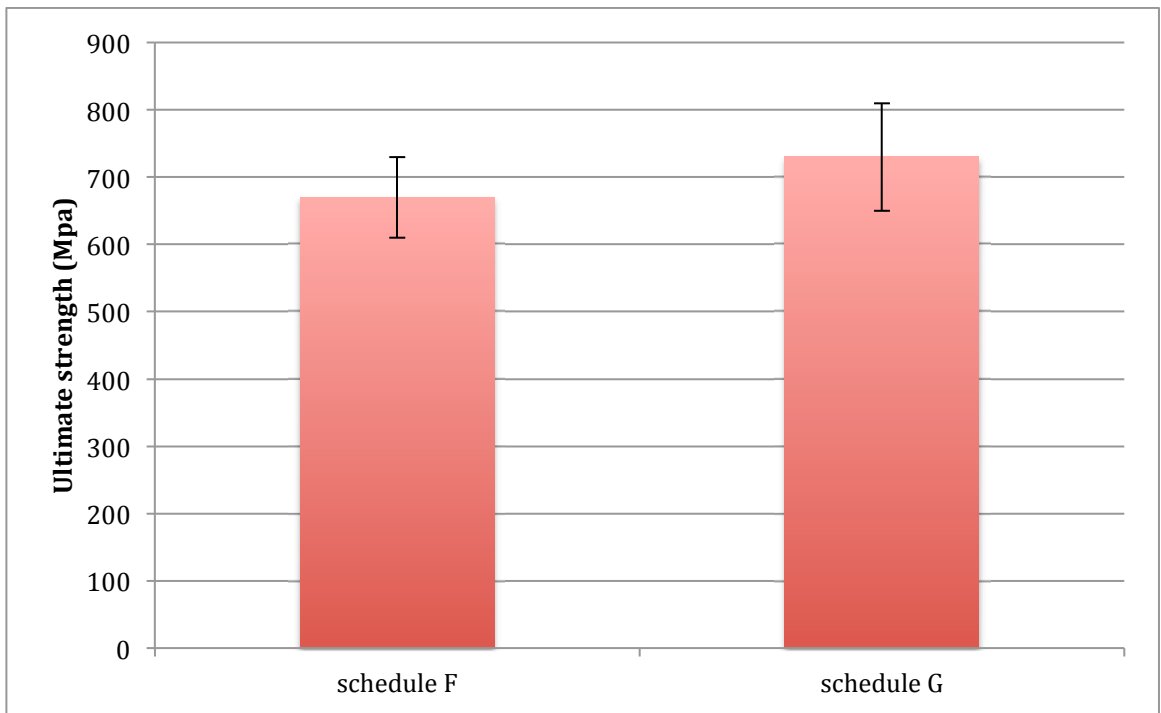
It was shown that the way of light curing of FRC and PFC play important role on final composite mechanical properties. It is well known that after the FRC light curing a small inhibited layer at the surface is created. Some of free radicals in this layer enable reaction with functional groups of PFC and chemical bonds are created. These bonds together with micromechanical bonds between the surface of PFC and FRC ensure the transfer of the load from PFC to FRC. However, if the FRC and PFC are cured at once, more direct chemical bonds is created between their surfaces. It leads to increasing of mechanical resistance, Young's modulus and ultimate strength of FRC/PFC, respectively. The comparison of  $E_C$  and  $\sigma_U$  of PFC/FRC cured at once or individually is shown in Fig. 39. Fracture surfaces of FRC/PFC composites cured at once are shown at Fig. 40.

**Table 12:** Comparison of Young's modulus and ultimate strength of PFU/C&B composites, sample preparation schedule F and G.

PFU/C&B composite (Arkona)	Young's modulus (GPa)	Ultimate strength (MPa)
sample preparation-schedule F	$18.1 \pm 1.7$	$670 \pm 60$
sample preparation-schedule G	$19.6 \pm 0.4$	$730 \pm 80$

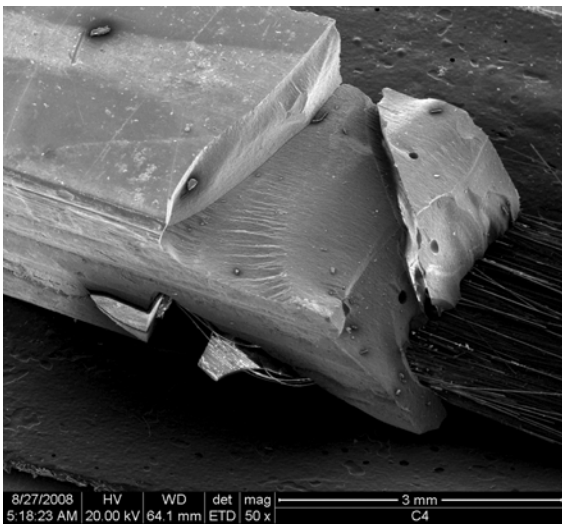


(a)

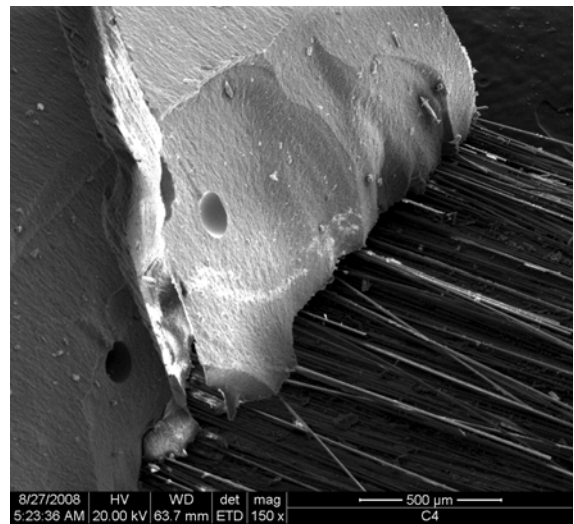


(b)

**Figure 39:** Comparison of Young's modulus (a) and ultimate strength (b) of PFU/C&B composites, sample preparation schedule F and G.



(a)



(b)

**Figure 40:** SEM photographs of PFU + Boston C&B composite fracture surfaces at 50x (a) and 150x (b) magnification after 3-point bending test, sample preparation – schedule G .

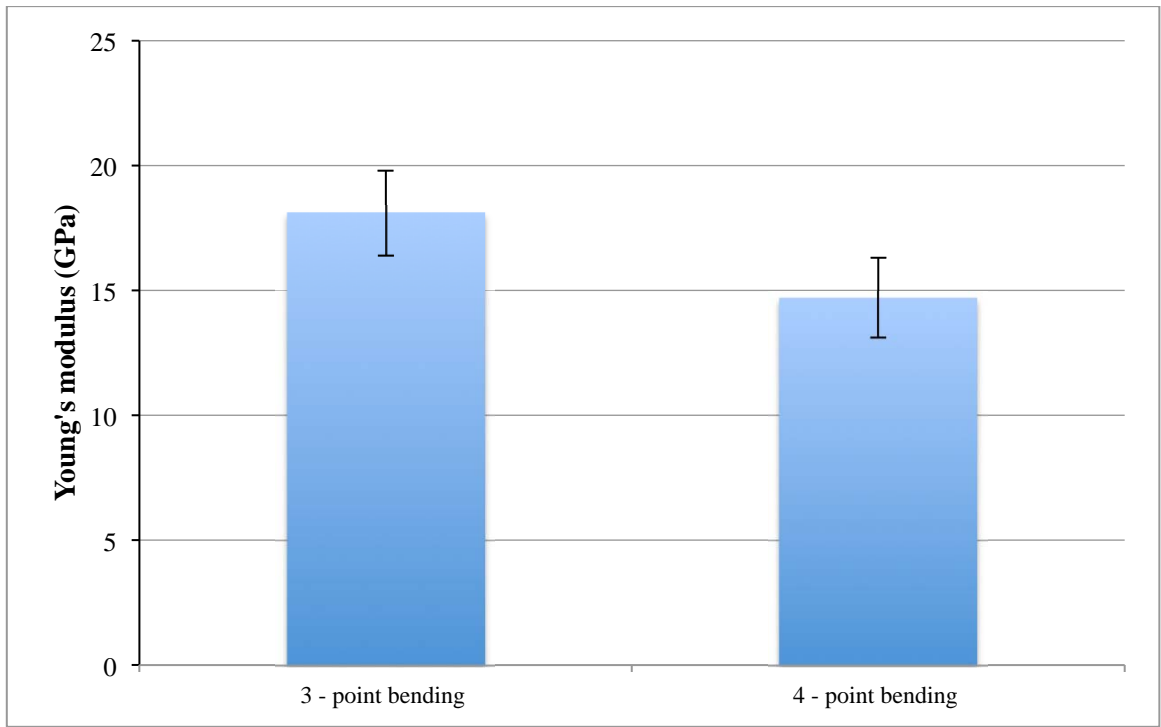
### 5.2.3 Young's modulus and ultimate strength in 4-point bending test

Four point bending tests were carried out to calculate Young's modulus ( $E_C$ ) and ultimate strength ( $\sigma_U$ ) and to compare different types of loading. The type of loading in 4-point bending test is closer to the physiological type of loading of dental bridges. PFU and C&B dental composites with PFU position at the bottom were tested and compared with the same type of specimens tested in 3-point bending mode. FRC strip was cured first and then placed in C&B composite.

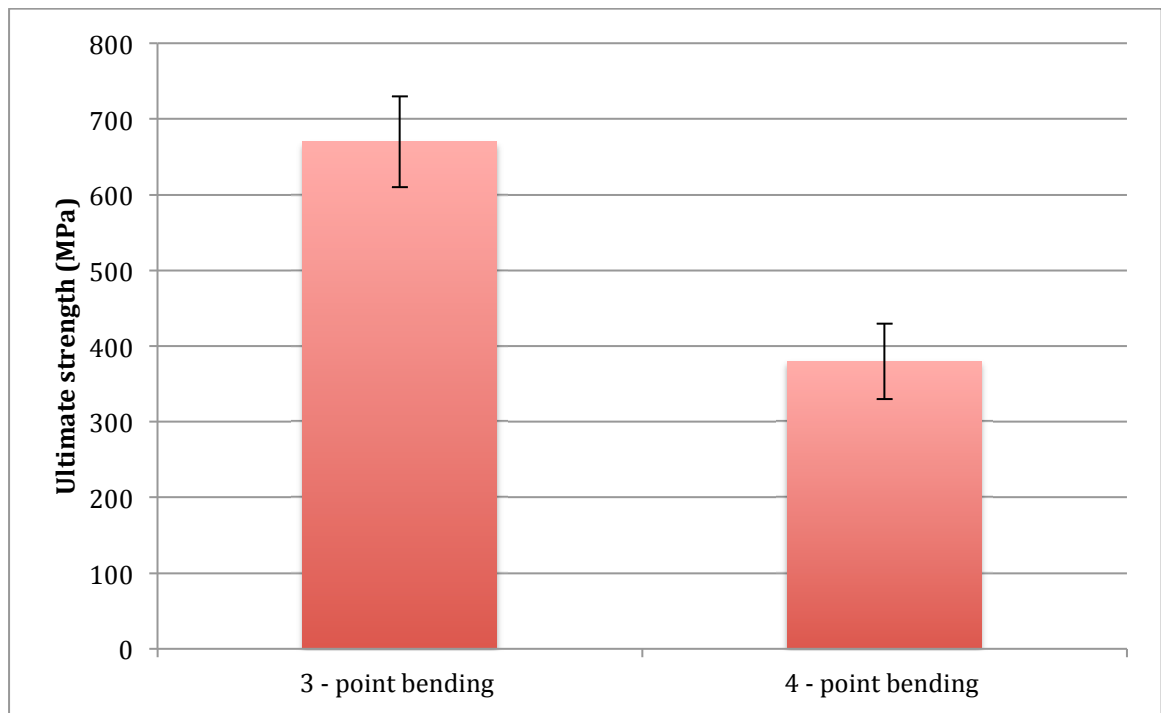
**Table 13.** Comparison of Young's modulus and ultimate strength of PFU/C&B composites, FRC in the bottom part, sample preparation – schedule F.

PFU/C&B composite (Arkona)	Young's modulus (GPa)	Ultimate strength (MPa)
3-point bending test	18.1 ± 1.7	670 ± 60
4-point bending test	14.7 ± 1.6	380 ± 50

The effect of different type of loading is apparent especially in higher values of ultimate strength in 3-point bending test. The influence on Young's modulus is insignificant. During the 4-point bending test the fibers start buckling in the middle of the specimen. Glass fibers are not able to resist this type of loading and the specimen will fracture. In 3-point bending test is in the middle of the specimen the loading bar that not allows this type of fracture and the specimen will fracture after exceeding the strength of fibers in tension.



(a)



(b)

**Figure 41:** Comparison of Young's modulus and ultimate strength of PFU/C&B composites, sample preparation – schedule F.

## 6 CONCLUSIONS

The influence of reinforcement of particulate composites with fiber composites used in dentistry was investigated. Adhesion strength between PFC and FRC was measured taking into account the way of PFC/FRC specimen preparation. The effect of different fiber reinforcement and the different position of FRC in PFC was also studied. Two types of dental FRC strips were used. One with unidirectionally oriented S2-glass fibers and the other with multidirectionally oriented E-glass fibers. Also two types of dental particulate composites were used. One was standard C&B composite and the other was low viscosity flow composite. For tests with interlayer an adhesive was used.

TGA analysis was used to determine the fiber content (wt.%) in FRC strips. Modified pull-out tests were carried out to measure the adhesion strength  $\tau_A$ . The static 3-point bending test was used to determine mechanical properties of PFC specimens reinforced with FRC strip. The static 4-point bending test was used to simulate the type of loading which is similar to the loading of dental bridge. SEM was used to describe the fracture surfaces of specimens. The conclusions of the work can be summarized as follows:

- 1) The fiber content was 55 wt.% for PFU strips and 60 wt.% for PFM strips, which is in good agreement with the data supplied by manufacturer. The diameter of the fibers used in PFU strip was approx.  $5\mu\text{m}$  and approx.  $9\mu\text{m}$  in PFM strip.
- 2) The type of sample preparation influenced the adhesion strength  $\tau_A$ . There was an increase of adhesion strength in the following consecution: samples with no interlayer, FRC cured first < samples with no interlayer, cured at once < samples with interlayer, FRC cured first.
- 3) The effect from point 2) was more apparent for samples with PFU strips and for samples where flow composite was used.
- 4) The increase of adhesion strength was insignificant for samples without interlayer where C&B composite was used.
- 5) The position of FRC component played very important role for increase of Young's modulus  $E_C$  and ultimate strength  $\sigma_U$ . Both of these values increased significantly in the following consecution: FRC in the upper part < FRC in the middle part < FRC in the bottom part. Which is in good agreement with theory [1]. The increase between FRC in the upper part and FRC in the lower part was nearly double for Young's modulus. The ultimate strength was more than 5 time higher.

- 6) The type of sample preparation (curing at once or separately) did not play any significant role for the value of Young's modulus and ultimate strength, respectively.
- 7) The ultimate strength is substantially higher in 3-point bending test in comparison to 4-point bending test.

There are two limit values of ultimate strength  $\sigma_U$ . The maximum  $\sigma_U$  exhibit unidirectionally oriented FRC loaded in tension. The second limit is the value of  $\sigma_U$  for multidirectionally oriented FRC loaded in compression. In reality, three types of stresses act on bi-material specimen. They are tension, compression and shear. The contribution of individual stresses depends on the position of the individual component in the specimen exposed to external loading. It was shown that for maximization of ultimate strength in bending of the bi-material specimen, the unidirectional FRC must be placed in the bottom part of PFC. The curing procedure (curing at once or separately) did not play any significant role for values of ultimate strength.

We can conclude that that using of fiber reinforcing strips is very important for using particulate composites in dental prosthetics. Using of this type of reinforcement will significantly improve the mechanical properties of such prepared devices and will prolong their operating live.

Using of such type of materials brings the opportunity for dentist to offer to their patients new, minimal invasive solution for their missing or mobile teeth.

## 7 LITERATURE

- [1] Piggott, M. R.: *Load Bearing Fibre Composites*. 2nd ed. New York: Kluwer Academic Publishers, 2002
- [2] Shao-Yun, F., Yiu-Wing, M., Lauke, B., Chee-Yoon, Y. *Mater. Sci. Eng. A* **232** (2002) 326 - 335
- [3] Y. Shan, Z., Liao, K. *Composites Part B* **32** (2001) 355 - 363
- [4] Ferracane, J. L.: *Materials in Dentistry: Principles and Applications*. 2nd ed. Baltimore: Lippincott Williams & Wilkins, 2001
- [5] Craig, R. G.: *Restorative Dental Materials*. 10<sup>th</sup> ed. St. Luis: Mosby-Year Book, 1997
- [6] Anusavice, K. J.: *Phillip's Science of Dental Materials*. Philadelphia: W. B. Saunders Company, 1996.
- [7] Craig, R. G.: *Dental Materials: Properties and Manipulation*. 6<sup>th</sup> ed. St. Luis: Mosby-Year Book, 1996.
- [8] Vallittu, P. K. *J. Prosthet. Dent.* **81** (1999) 318 - 326
- [9] Moszner, N., Salz, U. *Prog. Polym. Sci* **26** (2001) 535 - 576
- [10] Freilich, M. A.: *Fiber-Reinforced Composites in Clinical Dentistry*. Chicago: Quintessence Publishing Co., Inc., 2000
- [11] Çökeliler, D., Erkut, S., Zemek, J., Biederman, H., Mutlu, M. *Dental Materials* **23** (2007) 335-342
- [12] Kanie, T., Fujii, K., Arikawa, H., Inoue, K. *Dental Materials* **16** (2000) 150-158
- [13] Willems, G.: *Multi Standard Criteria for the Selection of Potential Posterior Composites*. Leuven: Khatolieke Universiteit te Leuven, 1992
- [14] Hellwig E., Klimek, J., Attin, T.: *Záchovná stomatologie a parodontologie*. Praha: Grada Publishing a. s., 2003
- [15] Callaghan, D. J., Vaziri, A., Nayeb-Hashemi, H. *Dental Materials* **22** (2006) 84-93
- [16] Goldberg, A. J., Burstone, C. J. *Dental Materials* **8** (1992) 197-202
- [17] Narva, K. K., Lassila, L. V. J., Vallittu, P. K. *Dental Materials* **21** (2005) 421-428
- [18] Garoushi, S., Vallittu, P. K., Lassila, L. V. J. *Dental Materials*, In Press, Corrected Proof, Available on-line 3 January 2007
- [19] Ladziesky, N. H., Chow, T. W., Ward, I. M. *Clin. Mater.* **6** (1990) 209 - 225
- [20] Ladziesky, N. H., Pang, M. K. M. Chow, T. W., Ward, I. M. *Aust. Dent. J.* **38** (1993) 28 – 38
- [21] Dyer, S., Lassila, L. V. J., Jokinen M., Vallittu, P. K. *Dental Materials* **20** (2004) 947-955

- [22] Jancar, J., Dibenedetto, A. T.: *Fiber Reinforced Thermoplastic Composites for Dentistry*. Berlin: Springer, 1992
- [23] Vallittu, P. K. *Journal of Prosthodontics* **5** (1996) 270-276
- [24] Nielsen L. E., Landel R. F., *Mechanical Properties of Polymers and Composites*, Marcel Dekker, New York, 1994
- [25] Nixdorf, K., Busse, G. *Comp. Sci. Tech.* **61** (2001) 889 – 894
- [26] Piggott, M. R.: *Load Bearing Fibre Composites*. 1st ed. New York: Pergamon Press, 1980
- [27] Jancar, J.: *Úvod do materiálového inženýrství kompozitů*. Brno: Faculty of Chemistry, 1999
- [28] Holmes G. A., Feresenbet E., Raghavan D., *Compos. Interfaces*, v. 10, **2003**, p. 515
- [29] Narkis M., Chen J. H., Pipes R. B., *Polym. Compos.*, v. 9, **1988**, p. 245
- [30] Park S., Jin J., *J. Colloid Interface Sci.*, v. 242, **2001**, 174
- [31] Ishida H., *Controlled Interphases in Glass Fiber and Particulate Reinforced Polymers: Structure of Silane Coupling Agents in Solutions and on Substrates in The Interfacial Interactions in Polymeric Composites* - Akovali G., Kluwer Academic Publishers, Dordrecht, 1993
- [32] Wu S., *Polymer Interface and Adhesion*, Marcel Dekker, New York, 1982
- [33] Dutschk V., Pisanova E., Zhandarov S., Lauke B., *Mech. Compos. Mater.*, v. 34, **1998**, p. 309
- [34] Hoecker F., Karger-Kocsis J., *J. Appl. Polym. Sci.*, v. 59, **1996**, p. 139
- [35] Petrie E. M., *Handbook of Adhesives and Sealants*, McGraw-Hill, New York, 2000
- [36] Lipatov Y. S., *Polymer Reinforcement*, ChemTec Publishing, Ontario, 1995
- [37] Comyn J., *Adhesion Science*, The Royal Society of Chemistry, Cambridge, 1997
- [38] Hull D., Clyne T. W., *An Introduction to Composite Materials*, Cambridge University Press, Cambridge, 1996
- [39] Wightman J. P., *Reinforcing Fibers for Composites in The Interfacial Interactions in Polymeric Composites* - Akovali G., Kluwer Academic Publishers, Dordrecht, 1993
- [40] Hull D., Clyne T. W., *An Introduction to Composite Materials*, Cambridge University Press, Cambridge, 1996
- [41] Koberstein J. T., *Tailoring Polymer Interfacial Properties by End Group Modification in Polymer Surfaces, Interfaces and Thin Films* - Karim A., Kumar S., World Scientific Publishing, Singapore, 2000
- [42] DiBenedetto A. T., Lex P. J., *Polym. Eng. Sci.*, v. 29, **1989**, p. 543
- [43] Kim J. K., Mai Y. W., *Compos. Sci. Technol.*, v. 41, **1991**, p. 333
- [44] Yallee R. B., Young R. J., *Composites Part A*, v. 29, **1998**, p.1353
- [45] Johnson A. C., Zhao F. M., Hayes S. A., Jones F. R., *Compos. Sci. Technol.*, v. 66, **2006**, p. 2023
- [46] Rao V., Drzal L. T., *Polym. Compos.*, v. 12, **1991**, p. 48
- [47] Dai Y., Xing J., Ye L., Mai Y., *Compos. Interfaces*, v. 13, **2006**, p. 67
- [48] Lodge R. A., Bhushan B., *J. Dent. Res.*, v. 84, **2005**, p. 365
- [49] Park J., Shin W., Yoon D., *Compos. Sci. Technol.*, v. 59, **1999**, p. 355

- [50] Matinlinna J. P., Lassila L. V. J., Kangasniemi I., Vallittu P. K., *J. Dent. Res.*, v. 84, **2005**, p. 360
- [51] Holmes G. A., Feresenbet E., Raghavan D., *Compos. Interfaces*, v. 10, **2003**, p. 515
- [52] Stokes R. J., Evans D. F., *Fundamentals of Interfacial Engineering*, Wiley-VCH, New York, 1997
- [53] Pukánszky B., *Eur. Polym. J.*, v. 41, **2005**, p. 645
- [54] Nardin M., Schultz J., *Interactions and Properties of Composites: a) Fibre-Matrix Adhesion Measurements in The Interfacial Interactions in Polymeric Composites - Akovali G.*, Kluwer Academic Publishers, Dordrecht, 1993
- [55] Zhandarov S., Mäder E., *Compos. Sci. Technol.*, v. 65, **2005**, p. 149
- [56] Park S., Jin J., *J. Colloid Interface Sci.*, v. 242, **2001**, 174
- [57] Tsai H. C., Arocho A. M., Gause L. W., *Mater. Sci. Eng. A*, v. 126, **1990**, p. 295
- [58] Chen P., Lu C., Yu Q., Gao Y., Li J., Li X. , *J. Appl. Polym. Sci.*, v. 102, **2006**, p. 2544
- [59] Park J., Kim D., Kong J., Kim M., Kim W., Park I., *J. Colloid Interface Sci.*, v. 249, **2002**, p. 62
- [60] Williams J. G., James M. R., Morris W. L., *Composites*, v. 25, **1994**, p. 757
- [61] Mäder E., Pisanova E., *Macromol. Symp.*, v. 163, **2001**, p. 189
- [62] DiBenedetto A. T., *Mater. Sci. Eng. A*, v. 302, **2001**, p. 74
- [63] Williams J. G., Donnellan M. E., James M. R., Morris W. L., *Mater. Sci. Eng. A*, v. 126, **1990**, p. 305
- [64] Hoh K., Ishida H., Koenig J. L., *The Diffusion of Epoxy Resin into a Silane Coupling Agent Interphase in Composite Interfaces - Ishida H., Koenig J. L.*, North Holland, New York, 1986
- [65] Tanoglu M., Ziaee S., McKnight S. H., Palmese G. R., Gillespie jr. J. W., *J. Mater. Sci.*, v. 36, **2001**, p. 3041
- [66] Kim J., Mai Y., *Engineered Interfaces in Fiber Reinforced Composites*, Elsevier Science, Amsterdam, 1998
- [67] Suzuki N., Ishida H., *Macromol. Symp.*, v. 108, **1996**, p. 19
- [68] Hodzic A., Kim J. K., Stachurski Z. H., *Polymer*, v. 42, **2000**, p. 5701
- [69] DiBenedetto A. T., Huang S. J., Birch D., Gomez J., Lee W. C., *Compos. Struct.*, v. 27, **1994**, p. 73
- [70] Jancar J., DiBenedetto A. T., *J. Mater. Sci.-Mater. Med.*, v. 4, **1993**, p. 562
- [71] Jancar J., DiBenedetto A. T., Goldberg A. J., *J. Mater. Sci.-Mater. Med.*,
- [72] Harding P. H., Berg. J. C., *J. Appl. Polym. Sci.*, v. 67, **1997**, p. 1025